Journal of Environmental Radioactivity, vol. 298, p. 108089, August 2026

Secondary radioactive contamination from manure application: Transfer and excretion of ^{137}Cs and ^{40}K in cattle under chronic Intake

Philip Sorokin, Mikhail Shchukin, Tsydendamba Sodboev

Philip Sorokin (philip.sorokin@gmail.com), Mikhail Shchukin: Moscow State Academy of Veterinary Medicine and Biotechnology – MVA named after K. I. Skryabin. *Department of Radiobiology and Biophysics*. 23 Akademika Skryabina str., Moscow 109472, Russia.

Tsydendamba Sodboev: A.I. Burnasyan Federal Medical Biophysical Center FMBA. *Department of Clinical and Radiation Medicine*. 46 Zhivopisnaya str., Moscow 123098, Russia.

Highlights:

- Manure-mediated secondary ^{137}Cs contamination was modeled for croplands.
- ^{137}Cs transfer factors and concentration ratios were derived for cattle manure.
- Standard manure application was radiologically safe in modeled scenarios.
- Manure dumping, water discharge, or thermal processing can create hotspots.
- Renal and gastrointestinal ^{137}Cs excretion varies with feed type and diuresis.

Keywords: *secondary radioactive contamination; cattle; manure; cesium-137; transfer factors; excretion.*

https://doi.org/10.1016/j.jenvrad.2026.108089

Abstract

A radioecological field study was conducted in agroecosystems of the Bryansk Region with elevated ^{137}Cs soil contamination densities (178–616 kBq m^{-2}) during the long-term post-Chernobyl period. Activity concentrations and distributions of ^{137}Cs and ^{40}K were determined in soils, pasture herbage, feeds, milk, and excreta during housing and grazing periods. Herd-level excretion fluxes were quantified by gamma spectrometry, and quasi-steady-state conditions were verified using mass-balance assessment. Empirical ratio-based transfer parameters (transfer factors and concentration ratios) were derived for ^{137}Cs in cattle manure, feces, and urine in the diet–product and soil–product pathways; corresponding parameters were also obtained for milk and pasture herbage. The parameters were compared with literature data and generic IAEA-based model calculations. A screening-level model was developed to estimate secondary ^{137}Cs contamination of soils after manure application to agricultural fields and private household plots, including the land area required for manure utilization. Scenario calculations indicated that manure processing and application at standard agronomic amounts over sufficiently large areas would result in limited radiological impact, even under relatively high radiocesium contamination. In contrast, localized manure accumulation, discharge into water bodies, traditional burning of dried manure, or thermochemical processing without effective off-gas cleaning may require separate risk assessment because these pathways can promote radiocesium redistribution and produce residues with elevated ^{137}Cs activity. At the herd level, ^{137}Cs was excreted through renal and gastrointestinal pathways in comparable proportions, with a modest predominance of gastrointestinal excretion. Potassium excretion was predominantly renal, indicating incomplete biokinetic similarity between cesium and potassium in cattle.

1. Introduction

More than four decades after the Chernobyl accident, previously restricted agricultural lands are increasingly being reconsidered for productive use. Although such reuse is important for rural economies, it may also create renewed radioecological risks. Even after radioactive decay and long-term fixation of radiocesium (^{137}Cs) in soils, radionuclides may remain available for secondary redistribution when agricultural practices mobilize contaminated soil, biomass, ash, water, or organic wastes. In this context, modeling provides a tool for assessing radiological risks and determining whether a material, activity, or situation requires regulatory control or can be exempted from it.

Secondary radioactive contamination refers to the remobilization and redistribution of previously deposited radionuclides through atmospheric, hydrological, aeolian, and biogeochemical pathways. It may occur after wildfires, which enhance atmospheric resuspension (*Evangeliou et al., 2016*), through redistribution in rivers, water bodies, marine areas, and bottom sediments (*Gulin et al., 2013; Monte et al., 2006; Funaki et al., 2022*), by lateral migration within soils (*Ramzaev and Barkovsky, 2023*), or through erosion-driven transfer of contaminated soil into drainage networks (*Evrard et al., 2016; Chalaux-Clergue et al., 2024*). In agroecosystems, additional inputs may arise from the use of ash as fertilizer, because ash can concentrate radionuclides and return them to the soil–plant system (*Sedukova et al., 2019; Herzner et al., 2025*).

Livestock production represents another, less well-characterized pathway of secondary radionuclide redistribution. Grazing on contaminated land, followed by manure storage or application to arable fields or household plots, may reintroduce radionuclides into agricultural cycles (*Nishiwaki et al., 2016*) and create localized hotspots, especially in large high-density herds or private farming systems where manure is stored or applied locally. In parallel, contaminated forage can transfer radionuclides into livestock products, making milk and meat direct dietary exposure pathways for humans.

The organization of agricultural production may further facilitate this pathway. In full-cycle farms, livestock production and feed cultivation occur within the same system, whereas in incomplete-cycle systems manure may be transported to external crop farms, private fields, or household gardens. Manure generated by cattle, pig, and poultry production may also exceed the capacity of local land to receive it safely, thereby entering broader manure or compost markets. Under these conditions, radionuclides accumulated in manure can be redistributed beyond the original contaminated pasture or farm unit.

A particularly important scenario is grazing on remote or semi-natural contaminated lands, including meadows, forest-edge areas, and riparian zones. In temperate regions, the grazing period may last up to approximately 180 days. Although part of the manure is deposited directly on pastures, about half of the manure generated during grazing enters the agricultural cycle through manure management practices. Thus, pasture-based livestock management, while economically advantageous and beneficial for animal welfare, may create a human-mediated pathway for radionuclide migration from contaminated natural or semi-natural areas into cultivated agroecosystems.

In addition, dried animal dung is used as a traditional household fuel in some regions (*Stoner et al., 2021*). Alongside biogas production, thermochemical treatment methods such as direct combustion and pyrolysis are also being developed as promising approaches for energy recovery from manure (*Maj, 2022; Su et al., 2022*). If manure is contaminated with radionuclides, these practices require assessment as potential redistribution pathways through ash, combustion-derived particulate matter, or processed residues. Against this background, manure-mediated redistribution should be considered as a specific agricultural pathway of secondary radioactive contamination.

The migration of anthropogenic radionuclides through trophic chains has been extensively studied since the first large-scale fallout events associated with nuclear weapons testing and nuclear accidents (*IAEA, 2010; IAEA, 2021*). However, integrated *in situ* field studies under real farm conditions in highly contaminated areas remain rare because access to the limited number of operating livestock farms in such territories is restricted and, in many cases, radioecological monitoring datasets for the investigated agroecosystems are incomplete. At the same time, the accumulated literature on radionuclide transfer in agricultural animals provides a basis for renewed analysis of transfer parameters, excretion fractions, and manure-mediated secondary contamination.

For radiocesium, manure-mediated redistribution is closely linked to cattle biokinetics and to the competitive influence of potassium, its biological analog, within the soil–plant–animal pathway. Because total manure is a mixture of feces and urine, assessment of ^{137}Cs activity in manure requires quantification of the contribution of each excretion pathway. Reported ^{137}Cs transfer and excretion parameters in cattle differ markedly among studies, and this variability requires detailed evaluation as a basis for further research.

Despite the potential importance of manure-mediated redistribution, quantitative parameters describing secondary contamination from radionuclide-contaminated manure remain limited in the literature. Reliable determination of ^{137}Cs transfer to cattle milk and excreta requires characterization of radiocesium distribution in the soil profile, vegetation, daily ration, and excretion pathways.

Accordingly, the objectives of the present study were: (1) to quantify ^{137}Cs transfer along the soil–plant–animal–manure pathway, including transfer to milk, pasture herbage, and cattle excreta; (2) to characterize the distribution of ^{137}Cs and ^{40}K in soils, vegetation, and cattle excretion pathways under chronic intake conditions; and (3) to develop and evaluate a model for predicting manure-mediated secondary contamination of agricultural land using field-derived parameters, a generic IAEA-based approach, and literature data.

This integrated field study was designed to characterize current conditions in highly contaminated areas during the long-term post-Chernobyl period. It covered both housing and grazing management periods, allowing manure-mediated radiocesium transfer to be evaluated under contrasting feeding regimes. The results may support predictive assessments, contribute to rehabilitation strategies for agricultural lands in radioactively contaminated territories, and support efforts to reduce population radiation exposure and to manage environmental risks associated with potential secondary contamination.

2. Materials and methods

2.1. Study sites and experimental animals

The study was conducted in 2023–2024 on dairy cattle farms located in the Bryansk Region, within the zone of residence with the right to resettlement. The current mean ^{137}Cs soil contamination density at the study sites ranged from 178 to 616 kBq m^{-2}.

Group 1 was located in the village of Katashin and comprised Brown Swiss cattle. Group 2 was located in the village of Katichi and comprised Black-and-White cattle. The farms were situated 183–195 km from the Chernobyl Nuclear Power Plant (ChNPP) and 28 km from each other within a similar forest–steppe landscape (coniferous–broadleaf forests) dominated by soddy-podzolic soils (Fig. 1).

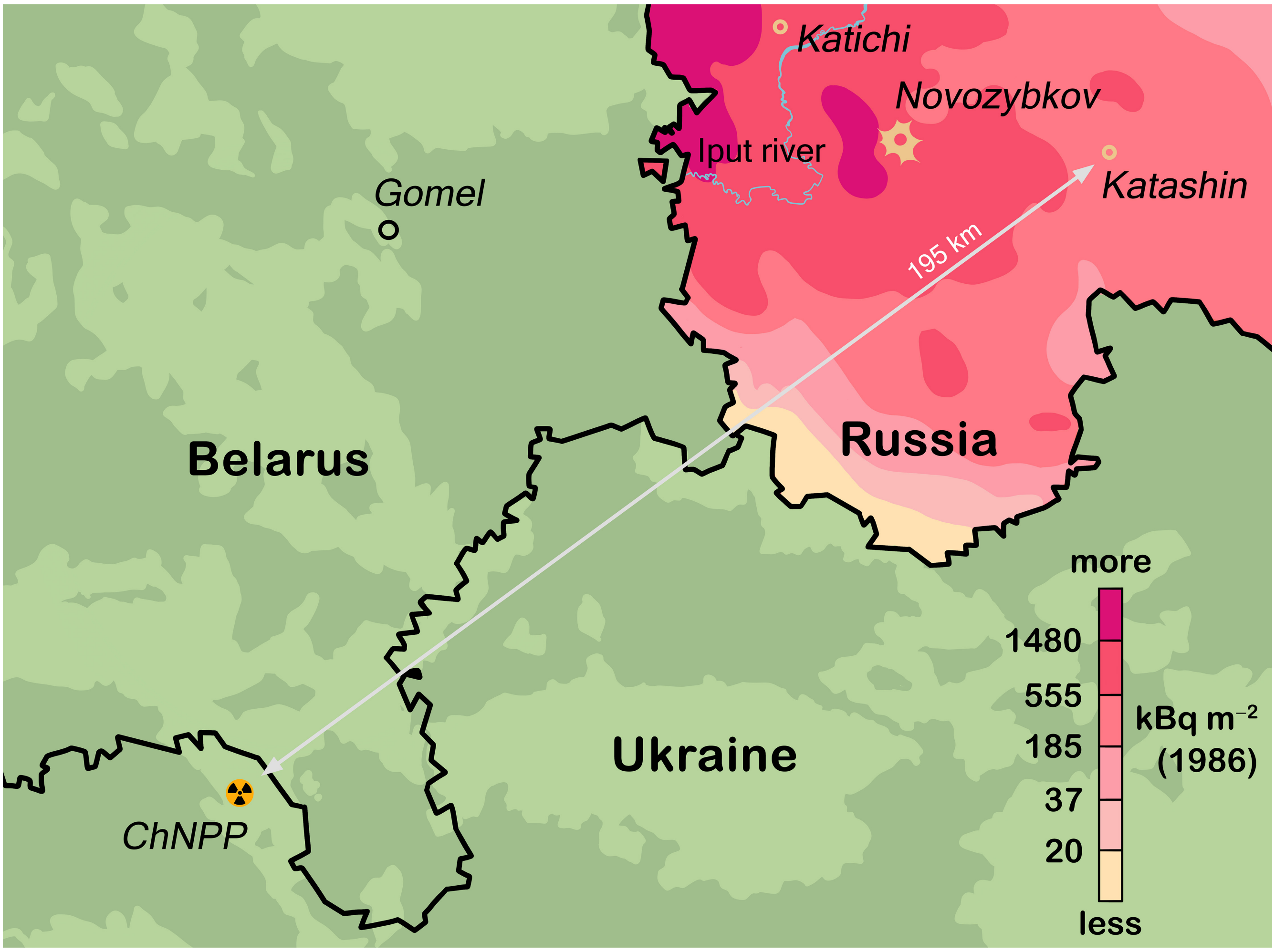

Fig. 1. ^{137}Cs soil contamination density in the Bryansk Region in 1986, based on soil-sample measurements supplemented by aerial survey data. Compiled from data reported by *Israel and Bogdevich (2009)*.

For each group and management period (housing and grazing), 20 clinically healthy lactating cows aged 4–6 years in mid-lactation were selected. The animals were maintained under standardized feeding and husbandry conditions. No bedding was used in the stalls, and no sorbents were administered in the diet. In all cases, sampling was conducted within a single 24-h period, during which one milk, urine, and fecal sample was collected from each selected animal. This design was appropriate for the herd-level objectives of the study, because all animals had been maintained on the same ration for at least 40 days before sampling, and the inclusion of 20 animals per group for each management period allowed individual variation to be averaged when estimating group-level transfer and excretion parameters under steady-state feeding conditions.

All procedures complied with applicable veterinary regulations and principles of humane animal treatment. The sampling was performed using non-invasive methods as part of routine farm management procedures, without additional stress or experimental irradiation. Because sampling was non-invasive and formed part of routine herd management, separate ethics approval was not required. All work was carried out in accordance with biosafety and radiation-safety requirements for handling samples and radioactive materials.

2.2. Instrumentation and sample analysis

The activity concentrations of ^{137}Cs and ^{40}K in milk, urine, and fecal samples from cattle, as well as in plant material, were determined by gamma spectrometry using an SKS-99 “Sputnik” spectrometer (*Amplituda Research & Technology Center LLC*) with a 500 cm^3 Marinelli beaker, corresponding to the certified measurement geometry implemented in the “Progress” software. The Marinelli beaker was filled completely with liquid samples or with homogenized, finely ground solid samples. Counting was performed with a NaI(Tl) scintillation detector in the manufacturer-supplied lead-shielded housing. According to the instrument specifications, the measurable activity range for ^{137}Cs was 3–10^4 Bq, and the basic relative measurement error did not exceed ± 10%.

Before each measurement series, the spectrometer was brought to operating conditions after a 15-min warm-up, and energy calibration was performed using a ^{22}Na reference source. A background spectrum was then recorded under the same measurement geometry for 60 min with an empty beaker and was used to account for the background contribution during data processing.

Sample spectra were acquired for 30 min. The activity concentrations of ^{137}Cs and ^{40}K were calculated in the “Progress” software based on calibration characteristics established for the certified geometry. Radionuclides were identified by their characteristic peaks at 661.7 keV (^{137}Cs) and 1460.8 keV (^{40}K).

Samples were dried in a drying oven at 105 °C to constant dry mass. Dry samples (plants, feces, and dry feeds) were homogenized by grinding to a finely ground, homogeneous fraction using an electric grinder. The equipment was thoroughly cleaned before each use to prevent cross-contamination.

Aboveground plant biomass (pasture herbage used as green fodder) was collected using the envelope (four corners and center) method at five points within an area of 10,000 m^2 (1 ha). The mass of each sample was 500–1000 g. Samples were cleaned of soil, washed with water, and dried. Activity associated with removable soil particles was accounted for separately through the estimated intake of ingested soil particles. Samples were weighed before and after drying to determine the dry-matter fraction.

Soil was collected at each plant-sampling point using a concentric soil corer with separation of soil horizons: 0–10, 10–20, and 20–30 cm. For determination of soil bulk density by horizon, samples were collected while preserving the porous structure. The mass of each sample was 1.5–2 kg. Horizon samples were dried and sieved through a laboratory sieve to homogenize the material and remove stones.

Urine and fecal samples were collected separately using a procedure similar to that described by *Bailoni et al. (2025)* and *Caprarulo et al. (2026)*. Sampling was performed during spontaneous urination and defecation using clean containers of adequate volume. Care was taken to prevent contact of the samples with feed, soil, excreta, the animal's hide, or other external contaminants.

Urine was collected into a sampling jar during spontaneous urination. Feces were collected during defecation by positioning a plastic shovel with an extended handle beneath the animal, followed by the immediate transfer of the material into a container. The mass of each sample was 1–2 kg. For moisture determination, fecal samples were weighed before and after drying to constant weight, and dry matter content was calculated from the loss in weight during drying. Milk was sampled manually during routine milking into 1 L plastic bottles. Milk and urine samples were analyzed without pretreatment.

Dry and conserved feeds for cows (hay, straw, silage, haylage) were collected on the farms during the housing period in winter. Composite samples for each feed type weighed 5–10 kg. Feed samples were analyzed without drying, and activity concentration values used for estimating daily radionuclide intake were expressed on a fresh-mass basis. Where conversion to dry mass was required for comparative calculations, the corresponding dry-matter fractions determined by sample weighing were applied.

2.3. Determination of soil contamination density

The ^{137}Cs contamination density (kBq m^{-2}) of soil plots (P) used for grazing and feed sampling was calculated using Equation 1:

$$P = \sum_{i=1}^{n} A_i \times \rho_i \times h_i \times 10^{-3} \qquad (1),$$

where:

n – number of soil horizons,
A_i – activity concentration of ^{137}Cs in soil horizon i (Bq kg^{-1}),
h_i – thickness (depth) of soil horizon i (m),
10^{-3} – conversion factor (Bq m^{-2} → kBq m^{-2}),
ρ_i – bulk density of soil horizon i (kg m^{-3}), calculated using Equation 2:

$$\rho_i = \frac{m}{S \times h_i} \times 10^3 \qquad (2),$$

where:

m – dry mass of the soil sample (g),
S – cross-sectional area of the sampler (cm^2),
h_i – thickness (depth) of the soil horizon (cm),
10^3 – conversion factor (g cm^{-3} → kg m^{-3}).

2.4. Calculation of transfer parameters of ^{137}Cs

Transfer factors (TFs) of ^{137}Cs from the daily ration (d kg^{-1} or d L^{-1}) to cattle milk (F_m) and excreta were calculated using Equation 3:

$$TF = \frac{A_{material}}{I_{day}} \qquad (3),$$

where:

$A_{material}$ – activity concentration of ^{137}Cs in the fresh mass of material (Bq kg^{-1}),

I_{day} – ^{137}Cs total activity in the daily ration (Bq d^{-1}).

Concentration ratios (CRs) of ^{137}Cs (dimensionless) from plant (pasture green herbage) to milk and excreta were calculated using Equation 4:

$$CR = \frac{A_{material}}{A_{plant}} \qquad (4),$$

where:

$A_{material}$ – activity concentration of ^{137}Cs in the fresh mass of material (Bq kg^{-1}),

A_{plant} – activity concentration of ^{137}Cs in the dry mass of plants (Bq kg^{-1}).

Aggregated transfer factors (T_{ag}) of ^{137}Cs (m^2 kg^{-1}) from the root-inhabited soil layer (0–20 cm) to cattle milk and excreta were calculated using Equation 5:

$$T_{ag} = \frac{A_{material}}{P_{soil}} \qquad (5),$$

where:

$A_{material}$ – activity concentration of ^{137}Cs in the fresh mass of material (Bq kg^{-1}),

P_{soil} – contamination density of ^{137}Cs in the 0–20 cm soil layer (Bq m^{-2}).

Aggregated transfer factors of ^{137}Cs (m^2 kg^{-1}) from the root-inhabited soil layer (0–20 cm) to plant (pasture green herbage) were calculated using Equation 6:

$$T_{ag} = \frac{A_{plant}}{P_{soil}} \qquad (6),$$

where:

A_{plant} – activity concentration of ^{137}Cs in the dry mass of plants (Bq kg^{-1}),

P_{soil} – contamination density of ^{137}Cs in the 0–20 cm soil layer (Bq m^{-2}).

Soil–plant (pasture green herbage) concentration ratio (F_v, dimensionless) relative to the standardized 0–10 cm soil layer was calculated using Equation 7:

$$F_v = \frac{A_{plant}}{A_{soil}} \qquad (7),$$

where:

A_{plant} – activity concentration of ^{137}Cs in the dry mass of plants (Bq kg^{-1}),

A_{soil} – activity concentration of ^{137}Cs in the dry mass of the 0–10 cm soil horizon (Bq kg^{-1}).

2.5. Mass balance and excretion fractions of ^{137}Cs and ^{40}K

Herd-level excretion fluxes under chronic intake of ^{137}Cs and ^{40}K (milk, urine, feces) were quantified in lactating cows during both the housing and grazing periods. The present study was designed as a farm-level mass-balance assessment rather than an individual metabolic-balance experiment. Although individual balance studies capture inter-animal variability, group-based fluxes provide robust estimates of radionuclide excretion through cattle milk and excreta under practical farm conditions and are consistent with the objectives of this work. Repeated sampling increased the number of group-level observations and allowed excretion to be assessed during grazing under natural conditions. Accordingly, the results are presented at the group level (mean fluxes and excretion fractions) and are not interpreted as individual kinetic parameters.

Reliability was assessed by verifying quasi-steady-state conditions using mass balance (Equation 8) for each group and period (housing and grazing). Under quasi-steady-state conditions, daily excretion is expected to approximately equal daily intake. Therefore, balance deviations of up to 20% were considered acceptable under semi-field conditions, and a mass balance of 80–120% was regarded as within the expected range and consistent with common practice (*Vogel et al., 2013*). Metabolic balance studies of radiocesium kinetics in cattle (Table 4) have reported mass-balance discrepancies of up to 26.7%, with a mean value of 12.7%.

$$B = \frac{E}{I} \times 100\% \qquad (8),$$

where:

I – daily intake of ^{137}Cs with the ration (Bq d^{-1}),

E – daily excretion of ^{137}Cs with milk (Bq d^{-1}), feces (Bq d^{-1}), and urine (Bq d^{-1}), calculated using Equation 9:

$$E = E_{milk} + E_{urine} + E_{feces} - A_{soil,ing} \quad (9).$$

During grazing, fecal ^{137}Cs excretion was corrected for the contribution of soil particles adhering to grazed herbage ($A_{soil,ing}$, Bq d^{-1}), because grazing cattle may ingest soil together with herbage, with mean soil intake representing approximately 3% of total dry matter intake (*Jurjanz et al., 2012*), and because chemically bound ^{137}Cs in mineral soils is assumed to be essentially unavailable for gastrointestinal (GI) absorption and thus excreted with the soil fraction (*Crout et al., 1993*).

This correction was applied to ensure consistency between the intake and excretion terms in the ration-based mass balance. In Equation 8, *I* represents daily ^{137}Cs intake with the measured ration and therefore excludes activity associated with soil that may be ingested during grazing. If this soil-derived component were retained in E_{feces}, it would artificially overestimate the fecal excretion fraction and, consequently, the apparent excretion balance for the grazing period. For the housing period, $A_{soil,ing}$ was set to zero because animals received harvested or mixed feed and did not ingest soil during feeding. This correction therefore allowed the housing and grazing periods to be compared on the same ration-derived intake basis. While it was applied to the mass-balance calculation and estimation of excretion fractions, it was not applied to the derivation of diet-to-manure transfer parameters, for which soil-derived activity was considered part of the total activity transferred to and excreted with manure.

Using the data shown in Tables 2 and 5, daily dry soil intake from the 0–10 cm layer was estimated at 412 g for Group 1 and 249 g for Group 2. Activity concentration of ^{137}Cs in pasture green forage was converted from a dry matter to a fresh matter basis using dry matter fractions of 0.25 (range, 0.19–0.32) for Group 1 and 0.15 (range, 0.13–0.20) for Group 2. Excretion fractions are presented for four group-period estimates, with the excretion fraction for compartment (i) calculated for each sampling round according to Equation 10:

$$F_i = \frac{E_i}{E_{milk} + E_{urine} + E_{feces,corr}} \times 100\% \quad (10),$$

where:

F_i – fraction of excretion via pathway (%),
E_i – daily activity excreted via pathway i (Bq d^{-1}),
E_{milk} – daily activity excreted in milk (Bq d^{-1}),
E_{urine} – daily activity excreted in urine (Bq d^{-1}),
$E_{feces,corr}$ – soil-corrected daily fecal activity excretion (Bq d^{-1}).

Mean daily milk yield was calculated as the ratio of the total milk volume in the bulk tank after morning and evening milking to the number of lactating cows in the barn. During housing, daily manure (total excreta) output per cow was calculated using Equation 11:

$$m_{excr} = \frac{V \times \rho}{N} \qquad (11),$$

where:

V – daily volume of excreta measured in the storage tank (m^3),
ρ – manure density (kg m^{-3}),
N – number of animals in the barn.

The mean excreta dry matter content was 0.13 (range, 0.11–0.16). The mean manure density was 1050 kg m^{-3} (range, 1015–1065 kg m^{-3}), consistent with the typical density of non-bedded semi-liquid manure. The partitioning of total excreted activity between urine and feces was estimated from individual observations of urination/defecation frequency and mass per event; the resulting urine-to-feces ratios were then averaged and applied to herd-level fluxes. For the calculation of milk mass and the activity concentrations of ^{137}Cs and ^{40}K in excreta, the densities of milk and urine were assumed to be 1030 and 1024 kg m^{-3}, respectively, corresponding to typical values for these fluids. For practical purposes, activity concentrations expressed in Bq L^{-1} were therefore considered approximately equivalent to those expressed in Bq kg^{-1}.

Milk secretion, urinary excretion, and fecal excretion represent the principal elimination pathways for ^{137}Cs in cows. By contrast, losses via the integumentary system, including the skin and associated structures such as hair, horns, and hooves, as well as via sweat, appear to be quantitatively minor and can therefore be neglected in biokinetic calculations. This interpretation is consistent with *Ilin and Moskalev (1957)* and *Pichl and*

Rabitsch (2003), who reported that the total activity associated with the externally contaminated integument accounted for less than 1% of total body activity in cattle.

2.6. Statistical processing and presentation of results

Statistical analysis included descriptive and nonparametric methods implemented using statistical software. Results are presented as mean ± standard deviation. To assess differences between soil sample datasets from different sites, the Kruskal–Wallis test was used because the Shapiro–Wilk test indicated deviation from a normal distribution. When the null hypothesis was rejected, post hoc pairwise comparisons were performed using Dunn's test with Bonferroni correction. The critical significance level was set at 0.05.

3. Results and discussion

3.1. Soil gamma-spectrometric characteristics

Table 1 summarizes the characteristics of the study plots and the bulk density values of the soil horizons calculated using Equation 2. Bulk densities in the 0–10 and 10–20 cm layers were within the expected range for these soil types. The higher bulk density in the 20–30 cm layer indicates subsoil compaction, likely associated with profile textural differentiation and, on arable plots, with plow-pan formation under conventional moldboard tillage. Table 2 presents the measured activity concentrations of ^{137}Cs and ^{40}K in the soil horizons of the study plots.

Table 1
Characteristics of soil plots in the experimental groups.

Plot				Soil type	Bulk density, g cm^{-3}		
No.	Group	Site type	Land use		**0–10 cm**	**10–20 cm**	**20–30 cm**
1	1	Meadow	Fallow arable land, pasture	Slightly podzolized soddy loam	1.53	1.61	1.81
2	2	Iput River floodplain	Virgin, pasture	Floodplain (alluvial) soddy loam	1.48	1.61	1.70
3		Meadow	Arable land, hayfield	Soddy-podzolic loam	1.63	1.65	1.73

Table 2
Activity concentrations of ^{137}Cs and ^{40}K (Bq kg^{-1}) in soil horizons, n = 5.

Horizon	Plot 1, group 1		Plot 2, group 2		Plot 3, group 2	
	^{137}Cs	^{40}K	^{137}Cs	^{40}K	^{137}Cs	^{40}K
0–10 cm	353 ± 107	416 ± 52	2266 ± 1372	137 ± 29	503 ± 81	370 ± 141
10–20 cm	373 ± 135	406 ± 79	1276 ± 952	167 ± 37	505 ± 79	298 ± 27
20–30 cm	353 ± 136	415 ± 72	440 ± 383	236 ± 120	276 ± 62	366 ± 38

Table 3 presents ^{137}Cs soil contamination densities calculated using Equation 1 for the integrated layers 0–10, 0–20, and 0–30 cm. In the 0–30 cm integrated layer, contamination densities ranged from 178 to 616 kBq m^{-2}.

Table 3
^{137}Cs soil contamination density in soil plots (kBq m^{-2}).

Plot No.	Group	Settlement	0–10 cm	0–20 cm	0–30 cm
1	1	Katashin	55	115	178
2	2	Katichi	336	541	616
3			82	166	214

3.2. Vertical distribution of radionuclides

Statistical analysis (k = 3 horizons, n = 5 replicates per horizon, N = 15 replicates per plot) demonstrated a uniform vertical distribution of ^{40}K across all plots throughout the soil profile (0–10, 10–20, and 20–30 cm).

On plot No. 1 (fallow arable land), the vertical distribution of ^{137}Cs was uniform over the entire soil profile. On plots No. 2 and No. 3, most of the ^{137}Cs inventory was concentrated in the 0–20 cm soil layer.

On plot No. 2 (virgin Iput River floodplain), ^{137}Cs activity decreased with depth: activity in the 0–10 cm layer was significantly higher than in the 20–30 cm layer. This pattern likely reflects continued radionuclide redistribution in the riverine environment, including transport with suspended sediments during floods.

On plot No. 3 (arable land), ^{137}Cs activity was uniform within the 0–20 cm plowed layer but significantly lower in the 20–30 cm subplow layer, consistent with repeated tillage to a uniform depth.

3.3. Horizontal distribution of radionuclides

Horizontal variability in the 0–20 cm layer was assessed by comparing the three plots (k = 3 plots; n = 10 replicates per plot; N = 30 replicates). For both ^{137}Cs and ^{40}K, activity concentration values did not differ significantly between plots No. 1 and No. 3.

The Iput River floodplain (plot No. 2) exhibited the highest ^{137}Cs activity. This pattern may reflect differences in post-accident land use and remediation history, together with continued ^{137}Cs redistribution within the river ecosystem.

The lower ^{40}K content on the virgin floodplain plot (No. 2) than on the arable plots (No. 1 and No. 3) may reflect both the contribution of potassium fertilization on agricultural land and the intrinsically lower potassium content of floodplain soddy soils derived from parent material poor in K-bearing minerals.

3.4. Literature review of Cs and K biokinetic studies in cattle

After absorption into the bloodstream, cesium is rapidly distributed among soft tissues, with skeletal muscle representing a major retention compartment. In cattle muscle, cesium loss is commonly described by one- or two-component kinetics; in the cattle data reviewed by *Fesenko et al. (2015)*, two-component fits gave fast-component biological half-lives (T_1) of approximately 3–22 days and slow-component biological half-lives (T_2) of about 36–84 days.

In lactating cows, *Hood and Comar (1953)* provided early tracer data on ^{137}Cs distribution and excretion after single oral and intravenous administration, showing substantial excretion via milk, urine, and feces over a 30-day period. *Sansom (1966)* subsequently showed that, after 28 days of continuous oral administration, whole-body retention of ^{137}Cs reached 5.7–8.2 times the daily administered activity. After intake ceased, milk activity declined rapidly during the initial phase, whereas the terminal phase was characterized by a half-life of about 30 days; muscle activity also declined slowly and eventually followed an exponential loss with a half-life of approximately 30–32 days.

For non-lactating cattle, including calves and beef animals, a longer effective half-life is expected because milk secretion does not contribute to elimination. In the calf experiments of *Sirotkin et al. (1972)*, whole-body elimination of ^{137}Cs after chronic administration was described by two components: 41% of the retained activity was eliminated with T_1 = 3.6 days, whereas the remaining 59% was eliminated with T_2 = 85 days. The upper end of the previously cited *Fesenko et al. (2015)* T_1 range (3–22 days), derived from *Iliazov (2001)* in a field feeding experiment with young bulls aged 10–12 months, appears to represent an exception within the broader dataset, but may still reflect a slower overall exponential loss expected in non-lactating animals.

The fractional GI absorption (f_1) of ^{137}Cs is generally high but depends on both the physicochemical form of the radionuclide and the type of feed. *Sansom (1966)* estimated f_1 in adult lactating cows at approximately 0.7–0.8 for soluble ^{137}Cs. *Howard et al. (2009)* summarized data on ^{137}Cs f_1 in adult domestic ruminants, giving a range of 0.67–0.93 with a mean of 0.8, while emphasizing that apparent absorption may be affected by endogenous secretion of absorbed ^{137}Cs back into the GI tract. In addition to diet-related factors, f_1 is age-dependent: in young animals it may be nearly complete, whereas lower absorption in adult ruminants is associated with maturation of GI function, reduced relative mineral demand, and the transition to a different feeding pattern (*Fesenko et al., 2007b*).

These differences in absorption, retention, and elimination determine the relative contribution of the main excretion pathways summarized in Table 4, which includes either cumulative recovery data after single-dose administration or chronic-intake experiments in which near-steady-state conditions were reported.

Table 4
Excretion fractions of cesium and potassium in ruminants and monogastric animals.

Species	Exposure source and administration route	Days after intake / collection period	n	Excretion fractions[a], %				Source
				Balance, %	Milk	Urine	Feces	
Cattle	Single (intravenous), tracer (^{137}Cs)	30 days	1	74.0	13.0 (17.6)	28.0 (37.8)	33.0 (44.6)	*Hood and Comar, 1953*
Cattle, sheep[b]	Single (oral), tracer (^{137}Cs)	30 days	1	89.0	9.6 (10.9)	39.0 (44.0)	40.0 (45.1)	
Rats, pigs[c]	Single (oral and intramuscular), tracer (^{137}Cs)	28 days	2	86.1	—	78.0 (90.6)	8.1 (9.4)	
Cattle	Single oral tracer dose in water (^{137}Cs)	32 days	1	96.1	7.5 (7.8)	17.6 (18.3)	71.0 (73.9)	*Ilin and Moskalev, 1957*
	Single (oral), tracer (^{134}Cs)	9 days	8	73.3	10.5 (14.3)	30.0 (41.0)	32.7 (44.7)	*Cragle, 1961*
	Single (oral), tracer (^{42}K)	66 h (~3 days)	8	49.2	4.2 (8.5)	38.0 (77.3)	~7.0[d] (14.2)	
	Dietary intake, alfalfa hay–grain ration, fallout (^{137}Cs)	4-day collection period	3	102.4	7.4 (7.2)	13.5 (13.2)	81.5 (79.6)	*Stewart et al., 1965*
	Dietary intake, alfalfa hay–grain ration (^{40}K)		3	93.2	11.9 (12.8)	62.4 (66.9)	18.9 (20.3)	

	Single (intravenous), tracer ($^{137}CsCl$)	7 days	2	90.8	14.5 (16.0)	32.0 (35.2)	44.3 (48.8)	*Sansom, 1966*
	Single (oral), tracer ($^{137}CsCl$) on cattle cake	28 days	4	99.9	8.7	37.6	53.7	
	Repeated (oral) for 28 days, twice daily, tracer ($^{137}CsCl$) on cattle cake	Last 7 days (mean)	4	87.7	7.9 (9.0)	25.5 (29.1)	54.3 (61.9)	
	Dietary intake, high *hay* ration for 10 days, fallout (^{137}Cs)	2-day collection period	8	—	5.4	16.7	77.6	*Johnson et al., 1968*
	Dietary intake, high *grain* ration for 10 days, fallout (^{137}Cs)			—	10.4	20.1	69.4	
	Dietary intake, high *hay* ration for 10 days (^{40}K)			—	6.9	84.3	8.6	
	Dietary intake, high *grain* ration for 10 days (^{40}K)			—	19.4	61.5	19.0	
	Continuous dietary intake, forage-based ration, twice daily, stable (K)	3–7 days collection period	16	98.0[e]	10.2 (10.4)	68.8 (70.2)	19.0 (19.4)	*Kume et al., 2004*
	Dataset-based study, stable (K)	—		—	—	64.0	15.4	*Marumo et al., 2024*

[a] Values in parentheses are projected fractions after normalization to 100% recovered excretion, assuming complete excretion balance. For *Johnson et al. (1968)*, total balance was not reported, but fractions sum to ~100%.
[b] Values are reported for cattle; sheep showed a similar excretion pattern.
[c] Values are reported for rats; pigs showed a comparable excretion pattern.
[d] Value estimated from graphical data.
[e] Fractions were calculated from the mean daily K balance reported for lactating cows.

Hood and Comar (1953) demonstrated interspecies differences in ^{137}Cs kinetics between monogastric and ruminant animals. In monogastrics, excretion was markedly shifted toward the renal pathway, whereas in ruminants the renal and GI fractions after a single dose were approximately equal. Similar excretion fractions in cattle were later reported by *Cragle (1961)*. By contrast, a marked shift of ^{137}Cs excretion toward the GI pathway was reported by *Ilin and Moskalev (1957)* and was also observed in studies of chronic dietary intake, particularly by *Stewart et al. (1965)* and *Johnson et al. (1968)*, and to a lesser extent by *Sansom (1966)*. Broadly similar excretion profiles were observed after oral and intravenous administration, although the relative urinary and fecal fractions differed between studies.

The study by *Johnson et al. (1968)* is notable as one of the few cattle metabolism studies conducted at the individual-animal level, with a comparatively large sample size (n = 8) and detailed reporting of feeding and housing conditions. The study also reports several relevant balance parameters, including milk yield, urine output, fecal water output, dietary intake, concentrations of both ^{137}Cs and K in milk, urine, and fecal water, and Ca, Mg, Na, and K concentrations in fecal water. The authors compared ^{137}Cs and K excretion under different dry-diet regimes. In our interpretation, these results suggest that reduced urinary potassium excretion was accompanied by redistribution toward the GI tract and milk, partly compensating for the reduction in the main urinary route. A similar increase in milk excretion was observed for ^{137}Cs, whereas the non-milk fractions changed only slightly.

The study by *Ilin and Moskalev (1957)* is of particular interest because ^{137}Cs was administered orally to cows in an aqueous form; therefore, feed-matrix effects on GI absorption should have been largely excluded, as in the tracer studies of *Hood and Comar (1953)*, *Cragle (1961)*, and *Sansom (1966)*. Nevertheless, under this exposure regime the authors indirectly estimated fractional GI absorption at approximately 50%, which appears atypically low for soluble ^{137}Cs, and reported a pronounced redistribution of ^{137}Cs recovery toward the fecal pathway. The magnitude of this shift was comparable to that observed by *Johnson et al. (1968)* under the high-hay and high-grain rations, despite the very different mode of administration. This pattern suggests that factors other than reduced dietary absorption alone, such as endogenous secretion of absorbed radiocesium into the GI tract or differences in renal elimination, may have contributed to the observed predominance of fecal recovery.

Across the literature, potassium excretion was predominantly renal, consistent with its near-complete GI absorption, reported to reach 99.9% (*Kume et al., 2004*). Such high absorption limits the fecal fraction, but this alone does not account for the contrasting excretion patterns of potassium and cesium. In most soluble-tracer studies with oral and intravenous administration summarized in Table 4, where feed-matrix effects on absorption were largely excluded, renal and GI excretion fractions of ^{137}Cs were comparable.

Johnson et al. (1968), in agreement with *Stewart et al. (1965)*, attributed the shift in ^{137}Cs excretion mainly to differences in GI absorption. *Sansom (1966)*, however, concluded that fecal predominance was not due to poor absorption, but rather to active secretion of absorbed radiocesium into the GI tract.

3.5. Cattle diet and excretion fractions of ^{137}Cs and ^{40}K

During the housing period, the diet was based on silage and haylage, with additional hay, compound feed (oats and rye), and straw. During the grazing period, the ration consisted primarily of pasture herbage and compound feed. The grazing season lasted approximately 6 months. Group 1 grazed on plot 1, whereas Group 2 grazed on plot 2; conserved forages for Group 2 were obtained from plot 3 (Table 1). The mean cow body weight was approximately 500 kg, and annual milk yield was about 5000 L. Table 5 presents the seasonal ration reconstructed on the basis of documented farm feeding records and seasonal feed consumption data, and cross-checked against official feeding recommendations (*Kalashnikov et al., 2003*).

Table 5
Estimated seasonal ration of the studied cattle, fresh mass (kg d^{-1}).

Diet	**kg d^{-1}**	**Period**
Pasture herbage Compound feed	55 4.5 (range, 3–6)	Grazing
Hay Straw Silage Haylage Compound feed	6 1 20 10 2 (0–2)	Housing
Mineral premixes Salt, buffer mixture	as required	All

Mean daily milk yield per cow was 10 L during housing and 17 L during grazing. Mean daily urine and fecal outputs were estimated at 20 kg per cow (range, 15–25 kg) and 35 kg per cow (30–40 kg), respectively, corresponding to a total excreta output of 55 kg per cow per day. These values were used as herd-level parameters for calculating ^{137}Cs and ^{40}K excretion fractions. Although total excreta output and the urine-to-feces ratio may vary among individual animals, the estimates were stable across the study groups and were consistent with both the reference range recommended for cattle manure-output calculations (*Ministry of Agriculture of the Russian Federation, 2024*) and literature values for lactating cows of 500 kg body weight at comparable milk yields (*Kormanovskii et al., 2017*). Table 6 presents the activity concentration of ^{137}Cs in feeds, milk, and excreta of lactating cows.

Table 6
Activity concentration of ^{137}Cs in feeds, milk, and excreta of cows (Bq kg^{-1}).

Material	**n**	**Group 1**		**Group 2**	
		Housing	**Grazing**	**Housing**	**Grazing**
Pasture herbage (dry mass)	20	—	153 ± 46	—	910 ± 374
Hay	10	45 ± 13	—	68 ± 23	—
Straw	10	33 ± 9	—	55 ± 18	—
Silage	10	21 ± 6	—	30 ± 7	—
Haylage	10	30 ± 8	—	38 ± 7	—
Compound feed	3	10 ± 3	8 ± 2	13 ± 2	15 ± 3
Milk	20	12 ± 2	21 ± 4	19 ± 4	65 ± 12
Urine	20	19 ± 5	39 ± 6	35 ± 5	135 ± 16
Feces (dry mass)	20	133 ± 41	210 ± 63	141 ± 33	1271 ± 313

The mean daily ^{137}Cs intake and excretion fluxes during the housing and grazing periods are summarized in Table 7. Mass balance was calculated according to Equation 8, while daily excretion was calculated using Equation 9. Daily intake was estimated from the data presented in Tables 5 and 6 for animals maintained on the same ration for more than 40 days before sampling. For the grazing period, daily excretion values were corrected for soil intake, as described in Section 2.5.

Table 7
Mean daily ^{137}Cs intake with feed and soil and excretion with milk, urine, feces (Bq d^{-1}).

Parameter	Group 1		Group 2	
	Housing	Grazing	Housing	Grazing
Intake with feed	1043	2140	1469	7575
Excretion (corrected)	1105	1947	1532	9024
Mass balance	106%	91%	104%	119%
Intake with soil	—	145	—	564

The calculations indicate that the system was close to a quasi-steady state, with excreted ^{137}Cs activity broadly corresponding to daily intake. The discrepancy between intake and excretion (excluding soil) ranged from 4% to 19%, supporting the internal consistency of the dietary assessment and the estimated daily outputs of milk, urine, and feces. Using Equation 10, excretion fractions of ^{137}Cs were calculated (Table 8).

Table 8
Excretion fractions of ^{137}Cs from the cattle body (%).

Material	Housing period		Grazing period		Mean	SD[a]	CV[b]
	Group 1	Group 2	Group 1	Group 2			
Milk	11	12	18	12	13	3.2	24%
Urine	34	46	40	30	38	7.0	19%
Feces	55	42	42	58	49	8.5	17%

[a] SD: Standard deviation.
[b] CV: Coefficient of variation.

On average across both groups, the ingested daily ^{137}Cs dose was excreted as 13% in milk (range, 11–18%), 38% in urine (30–46%), and 49% in feces (42–58%). After exclusion of non-cattle data from Table 4 and normalization to 100% for cattle studies with incomplete mass balance, the corresponding published cesium excretion fractions were 11% for milk (range, 5–18%), 31.0% for urine (17–44%), and 58% for feces (45–78%). Thus, the milk fraction observed here was very close to the literature mean. In Group 1, the milk fraction increased during grazing, when daily milk yield was also higher than during housing.

The urinary and fecal fractions also agreed with the literature values and remained within the published ranges for cattle. Overall, the observed distribution is consistent with individual balance studies in cattle, in which renal and GI excretion made broadly comparable contributions to total excreted activity (*Hood and Comar, 1953; Cragle, 1961; Sansom, 1966*). In the present study, GI excretion slightly exceeded renal excretion, but there was no marked predominance of the GI pathway. This contrasts with the stronger GI dominance reported by *Ilin and Moskalev (1957)*, *Stewart et al. (1965)*, and *Johnson et al. (1968)*. Among the chronic-intake studies summarized in Table 4, the results of *Sansom (1966)* were the closest to those obtained in the present study.

Ilin and Moskalev (1957) did not report the feeding and husbandry conditions in sufficient detail, which limits comparison with the present study. In contrast, the greater predominance of the GI pathway observed by *Stewart et al. (1965)* and *Johnson et al. (1968)* is most likely explained by the feeding regime, which was based on relatively dry, coarse feeds such as hay and grain. This type of diet was associated with lower GI absorption of ^{137}Cs, because roughages have relatively low absorption coefficients; however, it may also have been associated with lower water intake and reduced diuresis. Under such conditions, the renal contribution to ^{137}Cs elimination may decrease, with a corresponding increase in the relative importance of GI excretion.

By contrast, under grazing and silage-haylage feeding systems, higher water turnover and higher GI absorption coefficients for ^{137}Cs would be expected to favor a greater renal contribution and to limit any major shift toward GI excretion. During grazing, this effect may be further reinforced when the herbage contains forage species with diuretic properties, such as chicory and plantain. Dietary salt supplementation has likewise been reported to increase diuresis in cattle, by an average of 18.7% (*Letelier et al., 2024*), which we interpret as likely being mediated by increased water intake.

Urine output is closely related to dietary mineral–nitrogen load, especially Na, K, and N excretion in urine, and can be predicted from dry matter intake together with dietary Na, K, and N concentrations (*Bannink et al., 1999*). In this context, *Johnson et al. (1968)* and *Kume et al. (2004)* showed that daily urine output in cows was directly related to potassium intake and excretion, indicating that lower potassium turnover may be associated with reduced diuresis.

To compare ^{137}Cs with potassium, its biological analog, excretion fractions of ^{40}K were also calculated. Natural potassium contains ^{40}K together with the stable isotopes ^{39}K and ^{41}K, with an isotopic abundance of ^{40}K of approximately 0.0117%. This property underlies models of ^{137}Cs accumulation in plants (*Spirin et al., 2013*), in which the activity concentration of ^{40}K is used as an indicator related to exchangeable potassium in soil. As shown in Table 4, this approach is also widely used in animal balance studies to assess the excretion of stable potassium.

Table 9
Activity concentration of ^{40}K in milk and excreta of lactating cows (Bq kg^{-1}), n = 20.

Material	**n**	**Group 1**		**Group 2**	
		Housing	Grazing	Housing	Grazing
Milk	20	97 ± 20	132 ± 24	184 ± 44	96 ± 43
Urine	20	501 ± 204	456 ± 88	493 ± 201	281 ± 75
Feces (dry mass)	20	976 ± 252	436 ± 136	917 ± 149	716 ± 343

Excretion fractions of ^{40}K, calculated on the basis of the obtained data (Table 9) using Equation 10, are presented in Table 10. A potassium balance assessment was not performed because animals also received potassium with mineral premixes, and this contribution is difficult to quantify in semi-field conditions. Given the stability of the diet in the studied groups, potassium intake and excretion were considered balanced.

Table 10
Excretion fractions of ^{40}K from the cattle body (%).

Material	**Housing period**		**Grazing period**		**Mean**	**SD**	**CV**
	Group 1	Group 2	Group 1	Group 2			
Milk	6	12	17	16	13	5.0	39%
Urine	65	62	69	53	62	6.4	10%
Feces	29	26	14	31	25	7.6	30%

On average across the two groups, ^{40}K excretion occurred in the following fractions: 13% with milk (range, 6–17%), 62% with urine (53–69%), and 25% with feces (14–31%). These values confirm the predominance of the renal excretion pathway for potassium in cattle and are broadly consistent with the literature data summarized in Table 4. After normalization to 100% recovered excretion, the corresponding mean literature fractions were 12% for milk (7–19%), 70% for urine (62–84%), and 18.0% for feces (9–27%).

The mean milk excretion fractions of ^{137}Cs and ^{40}K were essentially the same, and their ranges overlapped. In both cases, the milk fraction increased during the grazing period, in parallel with higher milk yield. In contrast, the renal and GI excretion fractions of ^{137}Cs and ^{40}K did not overlap, demonstrating a much stronger predominance of renal excretion for potassium than for cesium.

The agreement between the observed and literature-derived potassium excretion fractions further supports the internal consistency of the estimated herd-level daily outputs of milk, urine, and feces. At the same time, the observed differences between potassium and cesium indicate that these elements, despite their biochemical similarity, are not fully biokinetically equivalent in cattle.

3.6. TFs and CRs of ^{137}Cs for cattle milk, excreta, and pasture herbage

^{137}Cs TFs are strongly influenced by soil and vegetation type, diet composition, and animal management practices. They are also affected by remediation measures, including potassium fertilization, liming, and other agrochemical countermeasures (*Fesenko et al., 2007a; Averin, 2020*). Despite the large body of data accumulated over several decades on the transfer of ^{137}Cs and other radionuclides to livestock products and pasture herbage, published TF values remain highly variable. For example, the geometric standard deviations reported for ^{137}Cs are 2.1 for cow milk, 2.4 for beef, and 4.1 for pasture herbage, resulting in differences of up to one to two orders of magnitude between the lower and upper bounds of reported TF ranges (Table 11).

Table 11
Published transfer parameters for ^{137}Cs transfer to cow milk, beef, and plant.

Transfer parameter		n	Arithmetic mean/value	Geometric mean	Minimum	Maximum	95th percentile
milk	F_m (d L^{-1})[a]	289	6.7×10^{-3}	4.9×10^{-3}	6.0×10^{-4}	5.7×10^{-2}	1.8×10^{-2}
	F_m (d L^{-1})[b]	21	9.8×10^{-3}	9.2×10^{-3}	—	—	1.3×10^{-2}
	CR (plant–milk)[a]	289	1.1×10^{-1}	8.4×10^{-2}	3.6×10^{-3}	9.0×10^{-1}	2.7×10^{-1}
	T_{ag} (m^2 kg^{-1})[c]	20	2.4×10^{-4}	—	—	—	—
	T_{ag} (m^2 kg^{-1})[c]	107	1.4×10^{-4}	—	—	—	—
	T_{ag} (m^2 kg^{-1})[d,e]	—	1.1×10^{-3}	—	—	—	—
	T_{ag} (m^2 kg^{-1})[d,f]	—	1.0×10^{-2}	—	—	—	—
beef	F_f (d kg^{-1})[d]	58	—	2.2×10^{-2}	4.7×10^{-3}	9.6×10^{-2}	—
	F_f (d kg^{-1})[b]	13	4.2×10^{-2}	3.8×10^{-2}	—	—	7.3×10^{-2}
	CR (plant–beef)[d]	17	2.3×10^{-1}	—	2.2×10^{-2}	7.3×10^{-1}	—
plant	*CR* (F_v), pasture[d,g]	124	—	1.9×10^{-1}	1.0×10^{-2}	2.6	—
	T_{ag} (m^2 kg^{-1}), grass vegetation[d,g,h]	4	4.0×10^{-3}	3.0×10^{-3}	1.0×10^{-3}	1.3×10^{-2}	—

[a] Source: *IAEA (2021)*.
[b] Source: *Fesenko et al. (2021)*. Based on Russian and Soviet data only.
[c] Source: *Travnikova et al. (2002)*. Remote Russian fallout-affected area, 1998–1999.
[d] Source: *IAEA (2010)*.
[e] Location: Iceland, 2001–2004.
[f] Location: Fennoscandia and northwest Russian Federation; early period after deposition.
[g] Values are given for loamy soil.
[h] Location: Alpine ecosystem.

Table 12 presents TFs from the daily ration to cattle milk (F_m) and excreta, calculated according to Equation 3. The obtained values are consistent with data reported by Russian and Soviet researchers, as summarized by *Fesenko et al. (2021)*. Compared with the *IAEA (2021)* cow milk dataset, the present F_m value was higher than the reported mean; however, it remains within the range of reported values and is well below the 95th percentile. TFs for total manure are reported here for the first time. For comparative analysis of the main excretion pathways, TFs to urine and feces are also presented, as these values may be relevant for selecting appropriate management or disposal strategies for liquid and solid manure fractions.

Table 12
^{137}Cs TFs (d kg^{-1} or d L^{-1}): daily ration → cattle milk (F_m) and excreta.

Material	Group 1		Group 2		Mean	SD	CV
	Housing	Grazing	Housing	Grazing			
Milk	1.2×10^{-2}	1.0×10^{-2}	1.3×10^{-2}	0.9×10^{-2}	1.1×10^{-2}	1.8×10^{-3}	16%
Urine	1.8×10^{-2}	1.8×10^{-2}	2.4×10^{-2}	1.8×10^{-2}	2.0×10^{-2}	3.0×10^{-3}	15%
Feces	1.7×10^{-2}	1.3×10^{-2}	1.2×10^{-2}	2.2×10^{-2}	1.6×10^{-2}	4.5×10^{-3}	28%
Manure	1.7×10^{-2}	1.5×10^{-2}	1.7×10^{-2}	2.0×10^{-2}	1.7×10^{-2}	2.1×10^{-3}	12%

During the grazing period, direct ration-based transfer estimates may be less straightforward because the amount of pasture herbage consumed can vary among animals and breeds. This variation depends on body weight, productivity, energy requirements, forage availability, and the nutritive value of the dominant plant species. Therefore, under chronic ^{137}Cs intake and after quasi-steady-state conditions have been reached, plant-to-material CRs provide an additional metric for describing transfer from feed to animal-derived materials. Table 13 presents the dimensionless CRs calculated for the grazing period using Equation 4.

Table 13
^{137}Cs CRs (dimensionless) during the grazing period: plant (dry mass) → product (fresh mass).

Material	Group 1	Group 2	Mean
Milk	1.4 × 10^{-1}	0.7 × 10^{-1}	1.1 × 10^{-1}
Urine	2.5 × 10^{-1}	1.5 × 10^{-1}	2.0 × 10^{-1}
Feces	1.8 × 10^{-1}	1.8 × 10^{-1}	1.8 × 10^{-1}
Manure	2.1 × 10^{-1}	1.7 × 10^{-1}	1.9 × 10^{-1}

Aggregated transfer factors (T_{ag}) provide another soil-based metric by relating the activity concentration in the material to the radionuclide inventory per unit area of soil. Table 14 presents T_{ag} values calculated for the soil-to-material pathway using the ^{137}Cs inventory in the 0–20 cm root-inhabited soil layer (Equations 5 and 6). This depth was selected because a previous analysis of soil horizons showed that ^{137}Cs contamination at the study plots was concentrated mainly within the 0–20 cm horizon, making this layer the most representative estimate of the integrated radionuclide inventory available to pasture plants.

For pasture herbage, Table 14 also presents the soil–plant CR (F_v), calculated for the standardized 0–10 cm soil layer (Equation 7). F_v is dimensionless and is based on the activity concentration of ^{137}Cs in pasture herbage on a dry-mass basis relative to that in soil on a dry-mass basis. Because radionuclide deposition density and soil activity concentrations are relatively well characterized in many countries, both aggregated TFs and F_v remain useful as screening-level tools. Some authors note (*IAEA, 2006*) that F_v may be less robust than T_{ag} when radionuclide contamination is heterogeneously distributed within the root-inhabited soil layer.

Table 14
Transfer parameters of ^{137}Cs during the grazing period: soil (dry mass) → material.

TF	Material[a]	Group 1	Group 2	Mean
T_{ag} (0–20 cm), $m^2\ kg^{-1}$	Milk	1.8×10^{-4}	1.2×10^{-4}	1.5×10^{-4}
	Urine	3.4×10^{-4}	2.5×10^{-4}	2.9×10^{-4}
	Feces	2.4×10^{-4}	3.1×10^{-4}	2.8×10^{-4}
	Manure	2.7×10^{-4}	2.8×10^{-4}	2.8×10^{-4}
	Pasture herbage	1.3×10^{-3}	1.7×10^{-3}	1.5×10^{-3}
F_v (0–10 cm), dimensionless	Pasture herbage	4.3×10^{-1}	4.0×10^{-1}	4.2×10^{-1}

[a] Pasture herbage is expressed on a dry-weight basis; the other materials are expressed on a fresh-weight basis.

For milk, the CR (plant-to-milk) and Tag (soil-to-milk) values obtained in the present study were very close to the corresponding mean literature values summarized in Table 11. For pasture herbage, comparison with published data for loamy soils showed a different pattern: the F_v value obtained here for the soil-to-plant pathway was higher than the reported mean, whereas the corresponding T_{ag} value was somewhat lower than the literature mean. Nevertheless, both plant-related parameters remained within the same order of magnitude as the published mean values. Given the broad reported ranges for these coefficients, this indicates that the observed soil-to-plant transfer to pasture herbage was broadly consistent with previous studies and can be considered comparable to the reported data.

The variability reported in the literature for diet-to-milk (F_m) and diet-to-meat (F_f) transfer, as shown in Table 11, is unlikely to be explained by fractional GI absorption alone, as supported by the excretion analysis presented in Sections 3.4 and 3.5. Although absorption is a key determinant of ^{137}Cs bioavailability, the subsequent distribution of absorbed radiocesium among milk, urine, feces, and soft tissues appears to be strongly influenced by animal-level physiological factors. In particular, differences in nitrogen and mineral metabolism, water intake, diuresis, lactation status, and housing or feeding conditions may alter the relative importance of renal, GI, and milk excretion pathways. Fecal excretion should also not be interpreted solely as the unabsorbed fraction of dietary ^{137}Cs, because it may include endogenous secretion of absorbed radiocesium back into the GI tract.

This interpretation provides a physiological basis for the wide variability of published TF values. Observed transfer factors may therefore reflect not only soil-to-plant transfer, dietary ^{137}Cs intake, and fractional absorption, but also the partitioning of absorbed radiocesium between excretion routes and body retention. Countermeasures such as Prussian blue, clay mineral binders including bentonite and zeolite, and other sorbents can effectively reduce radiocesium concentrations in livestock products by limiting bioavailability or enhancing GI elimination (*Zakharova et al., 2020; Oinuma et al., 2020*).

However, their effectiveness does not eliminate the need to understand the underlying animal-level mechanisms. Further research should therefore focus not only on external remediation strategies, but also on physiological factors controlling ^{137}Cs absorption, endogenous GI secretion, renal elimination, milk transfer, and tissue retention. Breed-related differences in these processes remain largely unexplored and may represent an additional source of variability in TF estimates.

3.7. Estimation of ^{137}Cs activity concentration in total manure

In the present study, the activity concentration of ^{137}Cs in fresh total manure was first estimated for each experimental group from the measured activities in feces and urine, weighted according to the relative fecal and urinary contributions to total manure. Based on these values, plant-to-manure CRs were calculated for the grazing period; these parameters relate the activity concentration in pasture herbage directly to the activity concentration in fresh total manure and therefore do not require knowledge of actual dry matter intake. In addition, diet-to-manure TFs were calculated from the daily ration and can therefore also be applied under mixed-feeding conditions during the housing period. A common advantage of both directly derived manure transfer parameters is that they provide activity concentration estimates per kilogram of fresh total manure without requiring estimates of daily excreta output or milk yield.

As an additional consistency check, comparative estimates were obtained using three IAEA-based models. Models 12 and 13 combined feed-to-product CRs with the corresponding diet-to-product TFs, together with the literature data on cesium biokinetics discussed above. These models are useful when the activity concentration of ^{137}Cs in pasture herbage is known, because they do not require direct information on either daily dietary activity intake or daily milk yield. Model 14 used the diet-to-milk TF within a complementary mass-balance approach for cases in which such intake and milk-yield data are available, with urinary and fecal excretion estimated as the difference between daily intake and activity excreted in milk.

$$A_{manure} = A_{feed} \times \frac{CR_{feed-beef}}{F_f} \times \frac{0.89}{m_{manure}} \qquad (12),$$

$$A_{manure} = A_{feed} \times \frac{CR_{feed-milk}}{F_m} \times \frac{0.89}{m_{manure}} \qquad (13),$$

$$A_{manure} = \frac{I_{day} \times (1 - F_m \times m_{milk})}{m_{manure}} \qquad (14),$$

where:

A_{manure} – activity concentration of ^{137}Cs in fresh total manure,

$CR_{feed–beef}$ – IAEA feed-to-beef concentration ratio, dimensionless (2.3×10^{-1}),

$CR_{feed–milk}$ – IAEA feed-to-milk concentration ratio, dimensionless (1.1×10^{-1}),

F_f – IAEA diet-to-beef transfer factor (2.2×10^{-2} d kg^{-1}),

F_m – IAEA diet-to-milk transfer factor (6.7×10^{-3} d L^{-1}),

A_{feed} – activity concentration of ^{137}Cs in pasture herbage, dry-mass basis (Bq kg^{-1}),

m_{manure} – daily fresh total manure output per cow (55 kg d^{-1}),

0.89 – mean literature-derived excretion fraction of ^{137}Cs via urine + feces (dimensionless),

I_{day} – daily dietary intake of ^{137}Cs (Bq day^{-1}),

m_{milk} – daily milk output per cow (10 and 17 kg d^{-1} during the housing and grazing periods, respectively).

The rationale for the approach used in Models 12 and 13 is that, when the activity concentration of ^{137}Cs in a livestock product, such as milk or meat, is known or estimated, the corresponding daily dietary intake of radiocesium can be back-calculated using the relevant IAEA diet-to-product TF. Under the quasi-steady-state conditions assumed in IAEA transfer models, this reconstructed intake can then be converted into the expected activity concentration in fresh total manure by multiplying it by the mean combined urinary and fecal excretion fraction of radiocesium, taken as 0.89, and dividing the result by the mean daily fresh total manure output per cow, assumed to be 55 kg. This reverse use of ratio-based transfer parameters is consistent with the general principles of IAEA transfer modeling, because it represents an algebraic rearrangement of the transfer-factor equation. However, it introduces an additional modeling step and therefore an additional source of uncertainty.

Table 15 presents the activity concentration of ^{137}Cs in fresh total manure estimated from measured fecal and urinary activities, weighted by their relative contributions to total manure. For comparison, it also reports estimates based on the mean manure TFs (diet–manure) and CRs (plant–manure) derived in the present study, as well as estimates obtained using the IAEA-based models. Models 12 and 13 were not applied to the housing period because the housing ration was mixed and included feed components with substantially different dry-matter contents. By contrast, Model 14 was applied to the housing period because it uses the known daily dietary activity intake directly.

Table 15
Activity concentration[a] of ^{137}Cs in fresh total manure during the management periods (Bq kg^{-1}).

Method	Grazing period		Housing period	
	Group 1	Group 2	Group 1	Group 2
Measured manure activity concentration	**32**	**155**	**18**	**25**
$TF_{diet–manure}$ (mean)	37 (+16%)	129 (–17%)	18 (0%)	25 (0%)
$CR_{plant–manure}$ (mean)	30 (–6%)	173 (+12%)	—	—
Generic Model 12 ($CR_{feed–beef}$ and F_f)	26 (–19%)	152 (–2%)	—	—
Generic Model 13 ($CR_{feed–milk}$ and F_m)	41 (+28%)	242 (+56%)	—	—
Mass-balance Model 14 (I_{day} and F_m)	35 (+9%)	122 (–21%)	18 (0%)	25 (0%)

[a] Values in parentheses indicate the relative deviation of the modeled values from the measured activity concentration, calculated as (modeled – measured) / measured × 100.

The calculated activity concentration values in total manure show that the estimates based on the mean manure TFs and CRs derived in the present study are generally consistent with the measured manure activity concentration values. The higher variability of the diet-to-manure TF during the grazing period likely reflects heterogeneity in green forage intake among groups. By contrast, during the housing period, when the ration was more constant, diet-to-manure TF showed substantially greater intergroup stability.

Among the IAEA-based model estimates, Model 12, based on beef transfer parameters, showed closer agreement with the measured manure activity concentrations than Model 13, based on milk transfer parameters. This difference likely reflects the different biological meaning of the two endpoints: beef activity integrates longer-term systemic retention of radiocesium, whereas milk activity is more sensitive to short-term variation in cesium partitioning among excretion pathways. The larger deviation of Model 13 therefore appears to be associated mainly with the reconstruction of intake from generic feed-to-milk transfer assumptions. By contrast, the Model 14 estimates, based on known daily dietary activity intake, were close to the manure activity concentrations calculated using the mean direct manure transfer parameters derived in this study, particularly the diet-to-manure TFs.

Overall, the results indicate that the IAEA transfer parameters for milk and beef perform well under long-term conditions and can be used in similar screening-level models, for example for assessing internal exposure doses from radiocesium. At the same time, it should be recognized that TFs to livestock products may vary depending on the phase of radioactive contamination and site-specific conditions, as shown in Table 11, which may affect model accuracy. In the subsequent calculations, the measured activity concentration values in total manure were used.

3.8. Prediction of secondary soil contamination from manure application

Secondary radioactive contamination resulting from the use of manure as fertilizer on croplands, including agricultural fields and private household plots, can be estimated using Equation 15. This general model predicts the increase in soil contamination density caused by the input of manure-derived ^{137}Cs:

$$\Delta P = \mu \times \frac{A_{p,manure}}{\omega} \times 10^{-3} \qquad (15),$$

where:

ΔP – increment in soil contamination density (kBq m^{-2}),
μ – amount of fresh or composted manure applied to soil (kg m^{-2}),
$A_{p,manure}$ – activity concentration of ^{137}Cs in fresh manure for the management period (Bq kg^{-1}),
ω – manure mass retention factor after storage or composting (1 for fresh; 0.25–0.9 for composted),
10^{-3} – conversion factor (Bq m^{-2} → kBq m^{-2}).

Equation 15 is based on the activity concentration of ^{137}Cs determined in fresh total manure. However, in practice, manure is often stored or composted before application. During composting, manure mass decreases because of water loss and organic matter decomposition. If ^{137}Cs is assumed to be conserved during this process, its total activity remains unchanged, whereas its activity concentration in the remaining material increases in proportion to the loss of mass.

The parameter ω accounts for this mass reduction and represents the fraction of the original fresh manure mass that remains after storage or composting before soil application. Thus, when $\omega = 1$, the material is fresh manure and no correction is applied. When $\omega = 0.7$, 70% of the original manure mass remains after storage or composting, and the activity concentration in the applied material becomes approximately 1.43 times higher than in fresh manure. Table 16 presents the increment in soil ^{137}Cs contamination density calculated using Equation 15 for composted manure ($\omega = 0.7$) applied at a typical amount ($\mu = 4$ kg m^{-2}).

Table 16
Increment in ^{137}Cs soil contamination density due to application of manure produced during each management period (kBq m^{-2}).

Period	Duration	Group 1	Group 2
Housing	183 days	0.10	0.14
Grazing	182 days	0.18	0.89

In the present analysis, manure was assumed to be incorporated within the cultivated topsoil layer, consistent with published manure incorporation practices ranging from shallow incorporation at approximately 6–8 cm to deeper strip-till placement at approximately 20–25 cm (*Pietzner et al., 2017*). Under these conditions, manure-derived ^{137}Cs may be more available for plant uptake than aged soil-bound radiocesium. On agricultural croplands, the potential transfer of manure-derived ^{137}Cs to crops may be reduced by regular agronomic practices, such as soil cultivation, liming, and fertilization. However, manure application on private household plots requires particular attention and risk assessment because edible crops grown on these plots may contribute directly to human dietary intake.

In this regard, the competitive interaction between potassium and cesium in plant transport systems is of interest when manure is applied to soil. Cattle manure contains substantial amounts of total potassium: *Marino et al. (2008)* reported 1.06–4.42 g K kg^{-1} fresh weight, equivalent to approximately 1.28–5.33 g K_2O kg^{-1} fresh weight. At a manure application amount of 4 kg m^{-2}, this corresponds to about 5.1–21.3 g K_2O m^{-2}, which is comparable to field-crop K_2O application amounts, typically ranging from approximately 6 to 22.5 g K_2O m^{-2} (*Jiang et al., 2018*).

From a practical perspective, manure heterogeneity and elemental distribution between fractions should be considered. Potassium in manure occurs predominantly in water-soluble and ionic forms, as supported by the relationship between K^+ and electrical conductivity in slurry systems (*Stevens et al., 1995*). Accordingly, potassium is expected to remain mainly associated with the liquid fraction after separation, whereas cesium may behave differently: based on differences in the fractional absorption and excretion of potassium and cesium in cattle, part of radiocesium may remain associated with solid organic components of feces and bedding material. Thus, cesium may be more strongly associated with the solid fraction.

Further research is needed to determine optimal management strategies for the liquid and solid manure fractions. When these fractions are applied separately, the application sequence may be important. If the liquid fraction, enriched in soluble potassium, is applied first, potassium may be taken up by plants before the main pool of cesium associated with the solid fraction enters the soil. In total manure, potassium and cesium enter the soil simultaneously, which may enhance their competitive interactions during root uptake. At the same time, bioavailable cesium introduced in the presence of mobile potassium may be partially fixed by soil minerals, potentially reducing its subsequent availability to plants. Exogenous sorbents applied before manure use may also help bind mobile cesium and reduce its bioavailability before the material enters the soil.

3.9. Potential risks of manure-mediated redistribution

One important manure-use pathway is the use of dried animal dung as household fuel. This practice is not merely an archaic residual behavior, but a persistent rural energy strategy in regions where access to wood, electricity, natural gas, or stable fuel markets is limited, and where livestock production provides a readily available combustible material (*Bharadwaj et al., 2025*). Millions of households in developing countries continue to burn dung cakes made from farmyard manure for domestic energy needs.

The environmental and health implications of this pathway are substantial. Combustion of dung fuel can generate very high indoor air pollution; for example, *Xiao et al. (2015)* reported 6-h average black carbon and PM2.5 concentrations of 24.5 and 873 μg m^{-3}, respectively, in a stone house using a chimney stove.

Epidemiological studies further associate biomass fuel use, including cow dung, with adverse health outcomes, such as respiratory symptoms in women who cook indoors (*Alim et al., 2014*), substantial particulate exposure in children even when they are not directly involved in cooking (*Devakumar et al., 2014*), and increased cataract risk among women exposed to household air pollution from solid-fuel combustion under poorly ventilated conditions (*Pokhrel et al., 2005*). In the latter study, animal dung was the predominant solid fuel, accounting for 78% and 64% of solid-fuel users in the two study groups, respectively, followed by wood at 19% and 36%.

Thus, the use of livestock manure as fuel should also be considered within the scope of radioecological assessment when the manure is contaminated with radionuclides, including in relation to potential combined effects (*Evstratova et al., 2023*). In such cases, combustion may create an additional pathway of secondary redistribution through ash and combustion-derived particulate matter, including indoor aerosols and emissions released outdoors through chimneys or ventilation. These assessments should therefore include not only manure application to soil, but also potential household exposure scenarios.

Improper manure disposal in agriculture includes direct discharge into surface waters (*Zhang et al., 2017*), accidental spills into streams (*Meade, 2004*), unprotected manure heap storage with subsequent leachate formation (*Kwon et al., 2017*), and infiltration from manure storage ponds, corrals, and manure-irrigated fields (*Harter et al., 2002*). Under vulnerable hydrogeological conditions, such as volcanic or karst aquifers, manure-derived contamination may also result from subsurface pathways. This includes illegal disposal of manure wastewater into lava caves, as shown for Jeju Island (*Kim et al., 2021*), as well as non-compliant effluent release from livestock farms into karst groundwater systems (*Pedrozo-Acuña et al., 2025*).

These scenarios are commonly associated with insufficient storage and treatment capacity, spatial concentration of livestock operations, a mismatch between manure production and the local assimilative capacity of land, poorly protected storage systems, and hydrogeological vulnerability. In addition to nitrogen, phosphorus, and organic loading, long-term or excessive manure use may be especially important as a source of Cu and Zn accumulation in soils and crops, reflecting the high excretion of these feed-derived trace elements with animal manure (*Zhang et al., 2017*). The pathways described above are general in nature and are considered here only insofar as manure contains residual radionuclide activity. Under such conditions, manure may act as a carrier of radionuclides, although their mobility will depend on element-specific speciation and soil interactions. This pathway may be particularly relevant for radiocesium because cesium is a biological and geochemical analog of potassium, a mobile plant nutrient involved in soil–plant transfer processes.

Temporary storage of tens to hundreds of tonnes of manure near livestock facilities is not uncommon, particularly before field application or further processing. When such material is concentrated on limited areas, even short-term stockpiling may create a risk of localized secondary contamination hotspots. This risk is governed by the activity concentration of ^{137}Cs in manure, the stored manure mass, the affected surface area, and the fraction of manure-associated activity transferred into the soil with the liquid phase.

For an illustrative weekly screening scenario for Group 2 during the grazing period, with a herd size of 210 head, approximately 40 t of fresh manure was assumed to accumulate locally, accounting for field losses or dispersion. The affected area was fixed at 50 m^2. The weekly increment in soil contamination density can be estimated using the area-based local-load model described by Equation 16:

$$\Delta P_{week} = \frac{A_{manure} \times m_{week}}{S} \times \eta_L \times 10^{-3} \qquad (16),$$

where:

ΔP_{week} – weekly increment in soil contamination density (kBq m^{-2}),
A_{manure} – activity concentration of ^{137}Cs in fresh manure for the period (Bq kg^{-1}),
m_{week} – weekly mass of fresh manure stored locally (kg),
S – affected surface area during local manure storage (m^2),
η_L – leachate-mediated transfer fraction of manure-associated ^{137}Cs entering the soil during one week of storage (dimensionless),
10^{-3} – conversion factor (Bq m^{-2} → kBq m^{-2}).

Using A_{manure} = 155 Bq kg^{-1}, m_{week} = 40 × 10^3 kg, S = 50 m^2, and η_L = 0.01, the estimated increment is $\Delta P_{week} \approx$ 1.2 kBq m^{-2} week^{-1}. This represents a low-end screening scenario, because the true value of η_L is currently unknown and may be higher depending on precipitation, manure moisture, storage duration, surface permeability, and the presence or absence of leachate collection. Defining a realistic range for η_L therefore requires further field-based investigation.

Safe utilization of manure from large livestock operations requires a sufficiently large land area. The required area for manure utilization by application to croplands can be calculated using Equation 17:

$$S = max\left\{\underbrace{\frac{qN\omega(365 - 0.5T_g)}{\mu}}_{Agronomic\ criterion}, \underbrace{\frac{qN[A_h(365 - T_g) + 0.5A_gT_g] \times 10^{-3}}{\Delta P_{max}}}_{Radiological\ criterion}\right\} \quad (17),$$

where:

S – required land area for utilization of the annual manure output (m^2),
q – daily fresh manure output per cow (kg d^{-1}),
N – total number of animals on the farm,
ω – manure mass retention factor after storage or composting (1 for fresh; 0.25–0.9 for composted),
365 – days per year,
0.5 – correction for manure losses on fields during the grazing period,
T_g – duration of the grazing period (d y^{-1}),
A_h – activity concentration of ^{137}Cs in fresh manure during housing (Bq kg^{-1}),
A_g – activity concentration of ^{137}Cs in fresh manure during grazing (Bq kg^{-1}),
μ – manure application amount per 1 m^2 of cropland (kg m^{-2}),
ΔP_{max} – maximum annual increment in contamination density (kBq m^{-2} y^{-1}),
10^{-3} – conversion factor (Bq → kBq).

The radiological criterion ΔP_{max} was defined as the threshold-based annual input of manure-derived ^{137}Cs that would prevent the long-term contamination density from exceeding the reference level. Repeated annual manure application results in cumulative input, whereas effective ecological removal progressively reduces the residual inventory. Therefore, ΔP_{max} was calculated from the reference contamination density and the effective loss rate of ^{137}Cs from the agroecosystem.

According to *IAEA (2010)*, an effective ecological half-time (T_{eff}) of 20 y, corresponding to the upper end of the reported long-term range (12–20 y), was used. The reference level was set at P_{ref} = 37 kBq m^{-2}, corresponding to the threshold above which territories are classified as radioactively contaminated and subject to radiological control in Russia and Belarus (*Russian Federation, 1991; Republic of Belarus, 2012*). Assuming first-order effective removal, the annual retention factor (r) is given by Equation 18.

$$r = 2^{-1/T_{eff}} \qquad (18).$$

Accordingly, to prevent the long-term manure-derived contamination density from exceeding the reference level P_{ref}, ΔP_{max} was calculated using Equation 19:

$$\Delta P_{max} = P_{ref} \times (1 - r) \qquad (19).$$

Using P_{ref} = 37 kBq m^{-2} and T_{eff} = 20 y gives ΔP_{max} = 1.3 kBq m^{-2} y^{-1}. This value was used as the radiological constraint for calculating the minimum land area required for manure utilization. Table 17 summarizes predicted scenarios for utilization of the annual output of composted unseparated manure from the experimental groups under different agronomic and radiological criteria, calculated using Equation 17. As noted above, daily fresh manure output was 55 kg per cow; Group 1 included 300 animals and Group 2 included 210 animals. A typical mass-retention factor for composted manure (ω = 0.7) was applied. During the 6-month grazing period, 50% of manure was assumed to be deposited directly on pasture and therefore unavailable for subsequent application to croplands.

Table 17
Predicted scenarios for cropland application of the annual total manure output from the experimental groups under different agronomic and radiological criteria (S, m^2).

Group	**Agronomic criterion (μ)**			**Radiological criterion (ΔP_{max})**
	4 kg m^{-2}	8 kg m^{-2}	10 kg m^{-2}	1.3 kBq m^{-2} y^{-1}
1	80 × 10^4	40 × 10^4	32 × 10^4	8 × 10^4
2	56 × 10^4	28 × 10^4	23 × 10^4	17 × 10^4

Scenario calculations using ΔP_{max} = 1.3 kBq m^{-2} y^{-1} indicated that the radiological land-area criterion did not exceed the agronomic requirement at any of the considered manure application rates. Thus, under the conditions and assumptions considered here, the application of manure to croplands can be regarded as a radiologically safe utilization pathway for ^{137}Cs.

Fig. 2 shows the modeled time course of manure-derived ^{137}Cs accumulation following repeated annual application under two scenarios: a model-derived input level of ΔP_{max} = 1.3 kBq m^{-2} y^{-1} and a higher input of 4.0 kBq m^{-2} y^{-1}. Under the higher-input scenario, the reference contamination density P_{ref} is reached after approximately 11 years. In contrast, under the ΔP_{max} scenario, the accumulated contamination density remains below P_{ref}, reaching only approximately 80% of this level after 46 years.

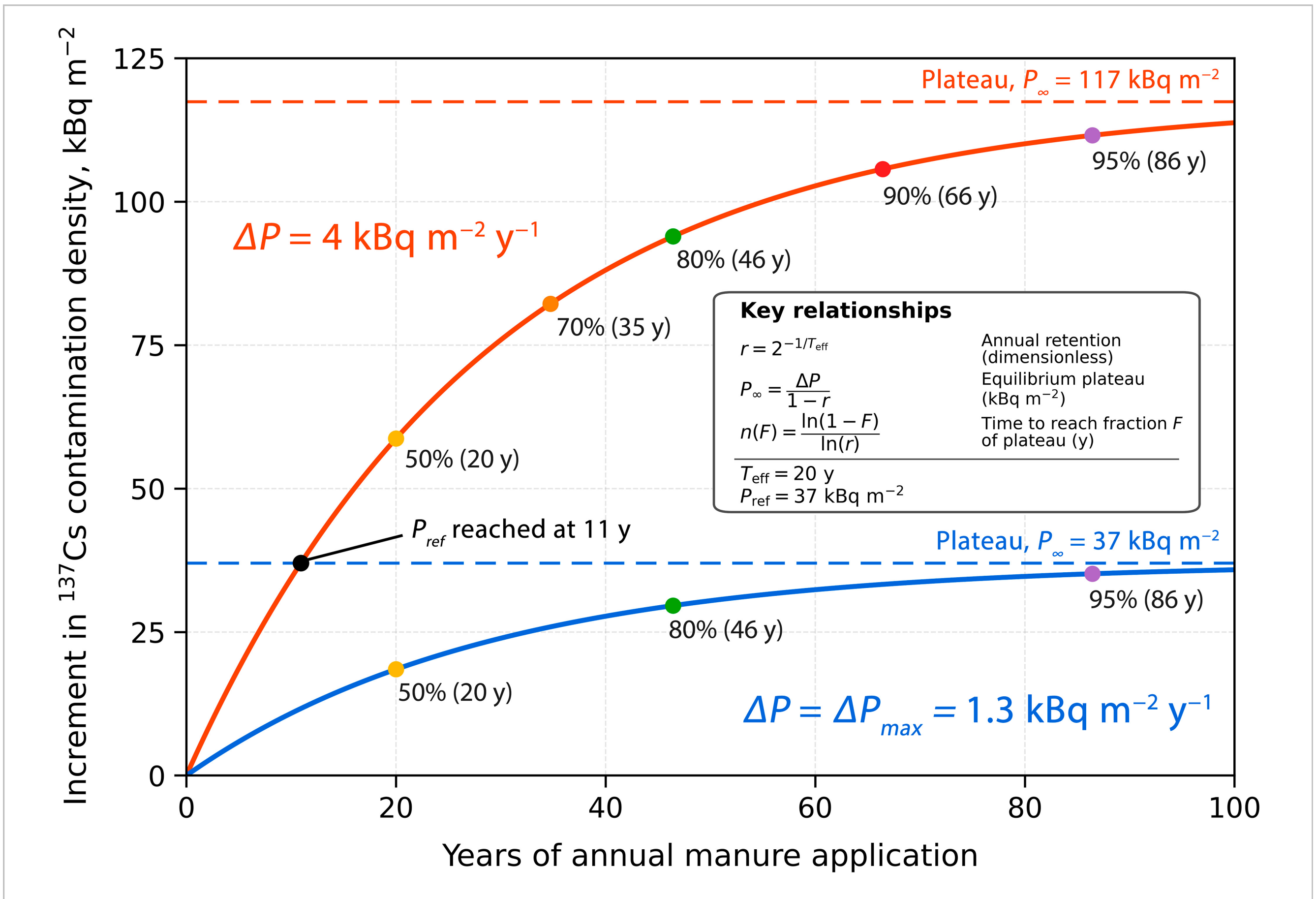

Fig. 2. Predicted accumulation of manure-derived ^{137}Cs contamination under threshold-based and excessive annual inputs.

For radionuclides with longer T_{eff} values, such as ^{90}Sr (20–30 y; IAEA, 2010), ΔP_{max} should be established separately, because long-term accumulation and redistribution among agroecosystem compartments become more important. The present assessment uses the reference contamination density as a benchmark for deriving ΔP_{max}; however, quantitative data on the transfer of bioavailable ^{137}Cs and other manure-associated radionuclides from manure-amended soils to crop plants remain limited. This need for caution is supported by the data summarized in Table 11, which indicate that soil-to-milk transfer coefficients during early stages after contamination may exceed long-term values by one to two orders of magnitude, suggesting greater bioavailability of recently deposited radiocesium.

An additional consideration is the soil-associated component of manure-mediated radionuclide transfer. In the present study, soil-derived activity entering manure through animal-mediated soil ingestion accounted for no more than about 7% of total ^{137}Cs activity. However, this pathway may be more important for particle-reactive radionuclides that are poorly transferred to livestock products but remain strongly associated with soil. In the 60-km zone around the ChNPP, this is particularly relevant for transuranic radionuclides, including plutonium and americium (*Nilova et al., 2019*), as well as for fuel-derived uranium oxide “hot” particles, which may persist in soils for decades and act as particulate carriers of actinides and fission products (*Poliakova et al., 2026*). Although plutonium and americium have much lower transfer coefficients to animal products than cesium (*IAEA, 2010*), grazing in undisturbed contaminated areas may promote the redistribution of both soil-bound radionuclides and fuel-derived particles to cultivated land through soil ingestion and subsequent excretion, especially with the solid manure fraction. This pathway may be relevant for household plots and other small-scale agricultural systems and should be considered in site-specific risk assessments.

4. Conclusions

Empirical ratio-based transfer parameters (transfer factors and concentration ratios) were derived for ^{137}Cs in cattle manure, feces, and urine in the diet–product and soil–product pathways. Corresponding parameters were also obtained for milk and pasture herbage. Together with an expanded literature analysis and generic IAEA-based model calculations, these results formed the basis of the proposed screening-level method for predicting secondary ^{137}Cs contamination of soils after manure application to agricultural fields and private household plots.

The present assessment indicates that manure management can represent a secondary pathway for the redistribution of ^{137}Cs in radioactively contaminated agroecosystems. Scenario calculations suggest, however, that processing and application over a sufficiently large land area, in accordance with technological standards and standard agronomic application amounts, can limit the resulting radiological impact even in areas with relatively high radiocesium contamination. Other manure-management scenarios may require separate risk assessment. Localized accumulation of large manure volumes, discharge into water bodies, or thermochemical conversion without effective off-gas cleaning may contribute to cesium redistribution and localized contamination. Such an assessment is also warranted for the traditional burning of dried manure, given potential human health implications, and for ash or other residues generated during manure processing for biofuel production, where ^{137}Cs activity may become elevated.

Secondary redistribution of manure-derived ^{137}Cs is governed not only by manure contamination levels, but also by manure-management practices, site-specific soil–plant transfer conditions, and the post-deposition stage, because transfer parameters may differ between early and long-term post-deposition periods. In contaminated areas, full-cycle livestock production should be preferred, with manure returned primarily to fields used for feed production for the same animals. This approach may reduce radionuclide redistribution from contaminated pastures or semi-natural grazing areas to external crop farms, household plots, or manure and compost markets. Careful selection of summer pastures is also important, especially where remote meadows, forest margins, floodplains, or riparian zones have elevated contamination levels.

On croplands, the impact of manure-borne ^{137}Cs may be moderated by dilution over larger areas and routine agronomic practices. Private household plots require particular caution because small application areas and local manure storage may enhance the relevance of plant uptake, especially given the potential bioavailability of manure-borne radiocesium. Direct consumption of locally grown crops may further increase the dietary significance of this pathway. In addition, radionuclides with low diet-to-animal transfer parameters may enter the agricultural cycle directly with soil particles adhering to manure or plant material, bypassing the diet–animal pathway.

Herd-level assessment of ^{137}Cs excretion under chronic intake, with verification of quasi-steady-state conditions, showed a modest predominance of GI over renal excretion (49% vs. 38%), with both pathways contributing substantially and comparably to total excreted activity. This partitioning is not fixed and may reflect not only GI absorption, but also water turnover, diuresis, and endogenous secretion of absorbed radiocesium into the GI tract, all of which may be influenced by feeding conditions and should be considered in further studies. Under silage–haylage and grazing feeding systems during the long-term post-Chernobyl period, no pronounced shift toward GI excretion was observed.

Comparison with ^{40}K confirmed that cesium and potassium are not fully biokinetically equivalent in cattle, as potassium showed a much stronger predominance of renal excretion than cesium. At the same time, the mean milk excretion fraction was essentially the same for ^{137}Cs and ^{40}K (13%), and for both elements the total fraction excreted with milk increased during grazing in parallel with higher milk yield. For both ^{137}Cs and ^{40}K, the observed excretion fractions were within published ranges, confirming the consistency of the excretion and balance estimates obtained in the present study.

The main uncertainties include inter-animal physiological variability, variation in feed intake and feed activity concentrations, estimates of daily excreta production, and gamma-spectrometric measurement error. However, the broad agreement between the field-derived estimates and the IAEA-based model calculations supports the plausibility of the derived transfer parameters and their use in assessing manure-mediated secondary contamination. This consistency also suggests that IAEA-based models, particularly those using diet-to-beef transfer parameters, may be useful for screening-level assessments in the long-term post-deposition period, as they showed good agreement with the empirical manure data.

Acknowledgements

The authors express their deep gratitude to Anatoly Aleksandrovich Kutuzov, chairman of SPK "Udarnik", and Viktor Mikhailovich Konokhov, chairman of SPK "Kolkhoz im. Lenina", the two agricultural production cooperatives where the study was conducted. Without their goodwill and assistance, this study would not have been possible. The comments of two anonymous reviewers are also highly appreciated.

References

Alim, A., Sarker, M.A.B., Selim, S., Karim, R., Yoshida, Y., Hamajima, N., 2014. Respiratory involvements among women exposed to the smoke of traditional biomass fuel and gas fuel in a district of Bangladesh. *Environ. Health Prev. Med.* 19 (2), 126–134. https://doi.org/10.1007/s12199-013-0364-4.

Averin, V.S., 2020. Basics of animal production under conditions of radioactive contamination. In: Strategies and practices in the remediation of radioactive contamination in agriculture. Report of a technical workshop, Vienna, 17–18 October 2016. International Atomic Energy Agency, Vienna, pp. 101–103.

Bailoni, L., Arango, S., Guzzo, N., Currò, S., Bianco, E., Simonetti, E., Zerbinati, E., Rainis, S., Sartori, C., 2025. Effect of a daily outdoor access on the urination and defecation behaviors and nitrogen excretion by lactating cows. *Front. Vet. Sci.* 12, 1429638. https://doi.org/10.3389/fvets.2025.1429638.

Bannink, A., Valk, H., Van Vuuren, A.M., 1999. Intake and excretion of sodium, potassium, and nitrogen and the effects on urine production by lactating dairy cows. *J. Dairy Sci.* 82 (5), 1008–1018. https://doi.org/10.3168/jds.s0022-0302(99)75321-x.

Bharadwaj, B., Dhungana, P., Ashworth, P., 2025. Burning dung cake as a household fuel: a review. *Next Energy.* 9, 100410. https://doi.org/10.1016/j.nxener.2025.100410.

Caprarulo, V., Scaglia, E., Simonetto, A., Ferronato, G., Sergi, V., Giagnoni, L., Gilioli, G., 2026. Modelling nitrogen excretion in dairy cows: an application to farms in the Po Valley (Italy). *Animals*, *16* (2), 294. https://doi.org/10.3390/ani16020294.

Chalaux-Clergue, T., Foucher, A., Chaboche, P.-A., Hayashi, S., Tsuji, H., Wakiyama, Y., Huon, S., Vandromme, R., Cerdan, O., Nakao, A., Evrard, O., 2024. Impacts of farmland decontamination on ^{137}Cs transfers in rivers after Fukushima nuclear accident: evidence from a retrospective sediment core study. *Sci. Total Environ.* 947, 174546. https://doi.org/10.1016/j.scitotenv.2024.174546.

Cragle, R.G., 1961. Uptake and excretion of cesium^{134} and potassium^{42} in lactating dairy cows. *J. Dairy Sci.* 44 (2), 352–357. https://doi.org/10.3168/jds.S0022-0302(61)89741-5.

Crout, N.M.J., Beresford, N.A., Howard, B.J., 1993. Does soil adhesion matter when predicting radiocaesium transfer to animals? *J. Environ. Radioact.* 20 (3), 201–212. https://doi.org/10.1016/0265-931X(93)90010-5.

Devakumar, D., Semple, S., Osrin, D., Yadav, S.K., Kurmi, O.P., Saville, N.M., Shrestha, B., Manandhar, D.S., Costello, A., Ayres, J.G., 2014. Biomass fuel use and the exposure of children to particulate air pollution in southern Nepal. *Environ. Int.* 66, 79–87. https://doi.org/10.1016/j.envint.2014.01.011.

Evangeliou, N., Zibtsev, S., Myroniuk, V., Zhurba, M., Hamburger, T., Stohl, A., Balkanski, Y., Paugam, R., Mousseau, T.A., Møller, A.P., Kireev, S.I., 2016. Resuspension and atmospheric transport of radionuclides due to wildfires near the Chernobyl Nuclear Power Plant in 2015: an impact assessment. *Sci. Rep*. 6, 26062. https://doi.org/10.1038/srep26062.

Evrard, O., Laceby, J.P., Onda, Y., Wakiyama, Y., Jaegler, H., Lefèvre, I., 2016. Quantifying the dilution of the radiocesium contamination in Fukushima coastal river sediment (2011–2015). *Sci. Rep.* 6, 34828. https://doi.org/10.1038/srep34828.

Evstratova, E.S., Geras'kin, S.A., Zhurakovskaya, G.P., Tolkaeva, M.S., Petin, V.G., 2023. General patterns of synergistic and antagonistic interactions in radiobiology. *"Radiation and Risk" Bulletin of the National Radiation and Epidemiological Registry*. 32 (2), 132–141. https://doi.org/10.21870/0131-3878-2023-32-2-132-141.

Fesenko, S.V., Alexakhin, R.M., Balonov, M.I., Bogdevitch, I.M., Howard, B.J., Kashparov, V.A., Sanzharova, N.I., Panov, A.V., Voigt, G., Zhuchenka, Y.M., 2007a. An extended critical review of twenty years of countermeasures used in agriculture after the Chernobyl accident. *Sci. Total Environ.* 383 (1–3), 1–24. https://doi.org/10.1016/j.scitotenv.2007.05.011.

Fesenko, S., Isamov, N., Barnett, C.L., Beresford, N.A., Howard, B.J., Sanzharova, N., Fesenko, E., 2015. Review of Russian language studies on radionuclide behaviour in agricultural animals: biological half-lives. *J. Environ. Radioact.* 142, 136–151. https://doi.org/10.1016/j.jenvrad.2015.01.015.

Fesenko, S., Isamov, N., Howard, B.J., Voigt, G., Beresford, N.A., Sanzharova, N., 2007b. Review of Russian language studies on radionuclide behaviour in agricultural animals: part 1. Gut absorption. *J. Environ. Radioact.* 98 (1–2), 85–103. https://doi.org/10.1016/j.jenvrad.2007.02.011.

Fesenko, S.V., Isamov, N.N., Prudnikov, P.V., Emlyutina, E.S., 2021. Radiological justification of reference levels of ^{137}Cs concentrations in fodder of agricultural animals. *Radiat. Biol. Radioecol.* 61 (6), 652–663. https://doi.org/10.31857/S0869803121060047. (In Russian).

Funaki, H., Tsuji, H., Nakanishi, T., Yoshimura, K., Sakuma, K., Hayashi, S., 2022. Remobilisation of radiocaesium from bottom sediments to water column in reservoirs in Fukushima, Japan. *Sci. Total Environ. 812*, 152534. https://doi.org/10.1016/j.scitotenv.2021.152534.

Gulin, S.B., Mirzoyeva, N.Yu., Egorov, V.N., Polikarpov, G.G., Sidorov, I.G., Proskurnin, V.Yu., 2013. Secondary radioactive contamination of the Black Sea after Chernobyl accident: recent levels, pathways and trends. *J. Environ. Radioact.* 124, 50–56. https://doi.org/10.1016/j.jenvrad.2013.04.001.

Harter, T., Davis, H., Mathews, M.C., Meyer, R.D., 2002. Shallow groundwater quality on dairy farms with irrigated forage crops. *J. Contam. Hydrol.* 55 (3-4), 287–315. https://doi.org/10.1016/s0169-7722(01)00189-9.

Herzner, V., Katzlberger, C., Pfeifer, C., Weigl-Kuska, M., 2025. Dose assessment for wood fuels and their ashes available in Austria. *Health Phys.* 129 (5), 388–398. https://doi.org/10.1097/hp.0000000000002018.

Hood, S.L., Comar, C.L., 1953. Metabolism of cesium-137 in rats and farm animals. *Arch. Biochem. Biophys.* 45 (2), 423–433. https://doi.org/10.1016/S0003-9861(53)80018-4.

Howard, B.J., Beresford, N.A., Barnett, C.L., Fesenko, S., 2009. Gastrointestinal fractional absorption of radionuclides in adult domestic ruminants. *J. Environ. Radioact.* 100 (12), 1069–1078. https://doi.org/10.1016/j.jenvrad.2009.03.023.

IAEA, 2006. Classification of soil systems on the basis of transfer factors of radionuclides from soil to reference plants. IAEA TECDOC-1497. International Atomic Energy Agency, Vienna, p. 113.

IAEA, 2010. Handbook of parameter values for the prediction of radionuclide transfer in terrestrial and freshwater environments. Technical Reports Series No. 472. International Atomic Energy Agency, Vienna.

IAEA, 2021. Approaches for modelling of radioecological data to identify key radionuclides and associated parameter values for human and wildlife exposure assessments. IAEA-TECDOC-1950. International Atomic Energy Agency, Vienna.

Iliazov, R.G., 2001. Obtaining of safe animal products in radioactive contamination area. *Vestn. RASHN*. 6, 82–83. (In Russian).

Ilin, D.I., Moskalev, Yu.I., 1957. On the metabolism of caesium, strontium and a mixture of β-emitters in cows. *J. Nucl. Energy*. 5 (3–4), 413–420. https://doi.org/10.1016/0891-3919(57)90042-6.

Israel, Y.A., Bogdevich, I.M., 2009. Atlas sovremennyh i prognoznyh aspektov posledstvij avarij na Chernobyl'skoj AJeS na postradavshih territorijah Rossii i Belarusi (ASPA Rossija–Belarus') [Atlas of modern and prognostic aspects of the consequences of the Chernobyl NPP accident on the affected territories of Russia and Belarus (ASPA Russia-Belarus)], Minsk. (In Russian).

Jiang, W., Liu, X., Wang, Y., Zhang, Y., Qi, W., 2018. Responses to potassium application and economic optimum K rate of maize under different soil indigenous K supply. *Sustainability*. 10 (7), 2267. https://doi.org/10.3390/su10072267.

Johnson, J.E., Ward, G.M., Firestone, E., Knox, K.L., 1968. Metabolism of radioactive cesium (^{134}Cs and ^{137}Cs) and potassium by dairy cattle as influenced by high and low forage diets. *J. Nutr*. 94 (3), 282–288. https://doi.org/10.1093/jn/94.3.282.

Jurjanz, S., Feidt, C., Pérez-Prieto, L.A., Filho, H.M.N.R., Rychen, G., Delagarde, R., 2012. Soil intake of lactating dairy cows in intensive strip grazing systems. *Animal* 6 (8), 1350–1359. https://doi.org/10.1017/S1751731111002734.

Kalashnikov, A.P., Fisinin, V.I., Shcheglov, V.V., Kleimenov, N.I. (Eds.), 2003. Normy i ratsiony kormleniya sel'skokhozyaistvennykh zhivotnykh: spravochnoe posobie [Feeding standards and rations for farm animals: reference book], third ed. Ministry of Agriculture of the Russian Federation, Moscow, p. 16. (In Russian).

Kim, S.H., Kim, H.-R., Yu, S., Kang, H.-J., Hyun, I.-H., Song, Y.-C., Kim, H., Yun, S.-T., 2021. Shift of nitrate sources in groundwater due to intensive livestock farming on Jeju Island, South Korea: with emphasis on legacy effects on water management. *Water Res.* 191, 116814. https://doi.org/10.1016/j.watres.2021.116814.

Kormanovskii, L.P., Tekuchev, I.K., Tekucheva, M.S., Chernovol, Yu.N., 2017. Scientific justification for determination of the daily output of cow excrement. *Russ. Agric. Sci.* 43, 53–56. https://doi.org/10.3103/S1068367417010128.

Kume, S., Nonaka, K., Oshita, T., Kozakai, T., Kojima, H., 2004. Potassium excretion of dry, pregnant and lactating cows fed forage. *Anim. Sci. J.* 75 (2), 179–184. https://doi.org/10.2508/chikusan.75.179. (In Japanese).

Kwon, M.J., Yun, S.-T., Ham, B., Lee, J.-H., Oh, J.-S., Jheong, W.-W., 2017. Impacts of leachates from livestock carcass burial and manure heap sites on groundwater geochemistry and microbial community structure. *PLoS One.* 12 (8), e0182579. https://doi.org/10.1371/journal.pone.0182579.

Letelier, P., Zanton, G.I., Wattiaux, M.A., 2024. Evaluation of protocols to determine urine output and urinary urea nitrogen excretion in dairy cows with and without dietary salt supplementation. *J. Dairy Sci.* 107 (9), 6742–6757. https://doi.org/10.3168/jds.2023-24075.

Maj, I., 2022. Significance and challenges of poultry litter and cattle manure as sustainable fuels: a review. *Energies*. 15 (23), 8981. https://doi.org/10.3390/en15238981.

Marino, P., De Ferrari, G., Bechini, L., 2008. Description of a sample of liquid dairy manures and relationships between analytical variables. *Biosyst. Eng.* 100 (2), 256–265. https://doi.org/10.1016/j.biosystemseng.2008.02.012.

Marumo, J.L., LaPierre, P.A., Van Amburgh, M.E., 2024. Urinary and fecal potassium excretion prediction in dairy cattle: a meta-analytic approach. *JDS Commun.* 5 (4), 272–277. https://doi.org/10.3168/jdsc.2023-0440.

Meade, R., 2004. Fish and invertebrate recolonization in a Missouri prairie stream after an acute pollution event. *N. Am. J. Fish. Manag.* 24 (1), 7–19. https://doi.org/10.1577/m02-094.

Ministry of Agriculture of the Russian Federation, 2024. RD-APK 1.10.15.02-17: Metodicheskie rekomendacii po tekhnologicheskomu proektirovaniyu sistem udaleniya i podgotovki k ispol'zovaniyu navoza i pometa [RD-APK 1.10.15.02-17: Methodological recommendations for the technological design of systems for manure and litter removal and preparation for use]. Moscow, p. 21. https://mcx.gov.ru/upload/iblock/a27/f20sl5akd8o65xztg8eob1ifzf6ooahh.pdf (accessed 20 May 2026). (In Russian).

Monte, L., Periañez, R., Kivva, S., Laptev, G., Angeli, G., Barros, H., Zheleznyak, M., 2006. Assessment of state-of-the-art models for predicting the remobilisation of radionuclides following the flooding of heavily contaminated areas: the case of Pripyat River floodplain. *J. Environ. Radioact.* 88 (3), 267–288. https://doi.org/10.1016/j.jenvrad.2006.02.006.

Nilova, E.K., Bortnovsky, V.N., Tagai, S.A., Dudareva, N.V., Zhukova, L.V., 2019. ^{241}Am on the territories adjacent to the Belarusian sector of the Chernobyl NPP resettlement zone: soil contamination, foodstuffs and population internal dose assessment. *Radiatsionnaya Gygiena = Radiation Hygiene.* 12 (2(св)), 75–82. (In Russian). https://doi.org/10.21514/1998-426X-2019-12-2s-75-82.

Nishiwaki, J., Asagi, N., Komatsuzaki, M., Mizoguchi, M., Noborio, K., 2016. Effect of added organic matter on soil fertility after stripping-off Cs-contaminated top soil at Iitate village in Fukushima Prefecture. *Paddy Water Environ*. 15 (1), 11–18. https://doi.org/10.1007/s10333-016-0524-4.

Oinuma, H., Saito, M., Oda, Y., Ajito, T., Abe, I., Hanada, M., 2020. Prussian blue in salt blocks decreases radiocesium activity concentration in milk from dairy cattle fed a diet contaminated by the Fukushima nuclear accident. *J. Environ. Radioact.* 222, 106307. https://doi.org/10.1016/j.jenvrad.2020.106307.

Pedrozo-Acuña, A., Ramírez-Salinas, N., Vázquez-Bustos, C., 2025. Water sustainability criteria to regulate the proliferation of pig farms on a karst aquifer. *Sustainability*. 17 (7), 3069. https://doi.org/10.3390/su17073069.

Pichl, E., Rabitsch, H., 2003. Activity levels of ^{137}Cs and ^{40}K in the skin and the cutaneous organs of a cow. *Health Phys.* 85 (2), 159–164. https://doi.org/10.1097/00004032-200308000-00004.

Pietzner, B., Rücknagel, J., Koblenz, B., Bednorz, D., Tauchnitz, N., Bischoff, J., Köbke, S., Meurer, K.H.E., Meißner, R., Christen, O., 2017. Impact of slurry strip-till and surface slurry incorporation on NH_3 and N_2O emissions on different plot trials in Central Germany. *Soil Tillage Res.* 169, 54–64. https://doi.org/10.1016/j.still.2017.01.011.

Pokhrel, A.K., Smith, K.R., Khalakdina, A., Deuja, A., Bates, M.N., 2005. Case–control study of indoor cooking smoke exposure and cataract in Nepal and India. *Int. J. Epidemiol.* 34 (3), 702–708. https://doi.org/10.1093/ije/dyi015.

Poliakova, T., Vlasova, I., Shiryaev, A., Kuzmenkova, N., Kalinichenko, S., Nikitin, A., Yapaskurt, V., Artemov, V., Chereslenko, E., Trigub, A., Bottomley, D., Kalmykov, S., 2026. Structural and isotopic peculiarities of a Chernobyl fuel "hot" particle. *J. Environ. Radioact.* 294, 107926. https://doi.org/10.1016/j.jenvrad.2026.107926.

Ramzaev, V.P., Barkovsky, A.N., 2023. Assessment of secondary radioactive contamination of a decontaminated land plot located on the territory of a recreation base in a wooded area. *Radiatsionnaya Gygiena = Radiation Hygiene*. 16 (2), 52–64. https://doi.org/10.21514/1998-426x-2023-16-2-52-64. (In Russian).

Republic of Belarus, 2012. On the legal regime of territories exposed to radioactive contamination as a result of the catastrophe at the Chernobyl Nuclear Power Plant: Law of the Republic of Belarus No. 385-Z dated 26 May 2012, as amended on 30 December 2022. Minsk. (In Russian).

Russian Federation, 1991. On social protection of citizens exposed to radiation due to the catastrophe at the Chernobyl Nuclear Power Plant: Law of the Russian Federation No. 1244-1 dated 15 May 1991, as amended on 25 December 2023. Moscow. (In Russian).

Sansom, B.F., 1966. The metabolism of caesium-137 in dairy cows. *J. Agric. Sci.* 66 (3), 389–393. https://doi.org/10.1017/S0021859600063693.

Sedukova, G.V., Isachenko, S.A., Timchenko, E.A., 2019. Use of wood ash as a fertilizer and ameliorant on the territory contaminated with radionuclides. *Arable Farming and Plant Breeding in Belarus*. 55, 87–93. https://earth.belal.by/jour/article/view/142/0?locale=en_US (accessed 20 May 2026). (In Russian).

Sirotkin, A.N., Sarapultsev, I.A., Panchenko, I.Ya., Shilov, V.P., Samarina, A.A., 1972. Kinetika obmena ^{137}Cs u krupnogo rogatogo skota: Biologicheskoe deistvie vneshnikh i vnutrennikh istochnikov radiatsii: sbornik rabot [Kinetics of ^{137}Cs exchange in cattle: Biological effect of external and internal sources of radiation]. Moscow, Meditsina [Medicine], 149–151. (In Russian).

Spirin, E.V., Anisimov, V.S., Dikarev, D.V., Kochetkov, I.V., Krylenkin, D.V., 2013. Forecasting model of transfer of ^{137}Cs to plants. *Radiat. Biol. Radioecol.* 53 (2), 199–205. https://doi.org/10.7868/S0869803113020094. (In Russian).

Stevens, R.J., O'bric, C.J., Carton, O.T., 1995. Estimating nutrient content of animal slurries using electrical conductivity. *J. Agric. Sci.* 125 (2), 233–238. https://doi.org/10.1017/S0021859600084367.

Stewart, H.F., Ward, G.M., Johnson, J.E., 1965. Availability of fallout Cs-137 to dairy cattle from different types of feed. *J. Dairy Sci.* 48 (6), 709–713. https://doi.org/10.3168/jds.S0022-0302(65)88325-4.

Stoner, O., Lewis, J., Martínez, I.L., Gumy, S., Economou, T., Adair-Rohani, H., 2021. Household cooking fuel estimates at global and country level for 1990 to 2030. *Nat. Commun.* 12, 5793. https://doi.org/10.1038/s41467-021-26036-x.

Su, G., Ong, H.C., Mohd Zulkifli, N.W., Ibrahim, S., Chen, W.-H., Chong, C.T., Ok, Y.S., 2022. Valorization of animal manure via pyrolysis for bioenergy: a review. *J. Clean. Prod.* 343, 130965. https://doi.org/10.1016/j.jclepro.2022.130965.

Travnikova, I.G., Shutov, V.N., Bruk, G.Ya., Balonov, M.I., Skuterud, L., Strand, P., Pogorely, Ju.A., Burkova, T.F., 2002. Assessment of current exposure levels in different population groups of the Kola Peninsula. *J. Environ. Radioact.* 60 (1–2), 235–248. https://doi.org/10.1016/s0265-931x(01)00106-0.

Vogel, H.G., Maas, J., Hock, F.J., Mayer, D. (Eds.), 2013. Drug discovery and evaluation: safety and pharmacokinetic assays, second ed. Springer Berlin, Heidelberg. https://doi.org/10.1007/978-3-642-25240-2.

Xiao, Q., Saikawa, E., Yokelson, R.J., Chen, P., Li, C., Kang, S., 2015. Indoor air pollution from burning yak dung as a household fuel in Tibet. *Atmos. Environ.* 102, 406–412. https://doi.org/10.1016/j.atmosenv.2014.11.060.

Zakharova, L.L., Zhorov, G.A., Dorozhkin, V.I., Obryvin, V.N., Brichko, N.A., 2020. Detoxication agents and technologies for animal husbandry under conditions of anthropogenic pollution. *BIO Web Conf.* 27, 00018. https://doi.org/10.1051/bioconf/20202700018.

Zhang, D., Wang, X., Zhou, Z., 2017. Impacts of small-scale industrialized swine farming on local soil, water and crop qualities in a hilly red soil region of subtropical China. *Int. J. Environ. Res. Public Health.* 14 (12), 1524. https://doi.org/10.3390/ijerph14121524.